To the Graduate Council:

I am submitting herewith a thesis written by Steven W. Moss entitled "Determination of Reentry Parameters During Descent from Low Earth Orbit." I have examined the final copy of this thesis for form and content and recommend that it be accepted in partial fulfillment of the requirements for the degree of Master of Science, with a major in Aerospace Engineering.

Dr. Firouz Shahrokhi, Major Professor

We have read this thesis and recommend its acceptance:

Charles T. N. Paludan

Michael J. Chaney

Accepted for the Council:

C W Minkel

Associate Vice Chancellor and
Dean of the Graduate School

STATEMENT OF PERMISSION TO USE

In presenting this thesis in partial fulfillment of the requirements for a Master's degree at The University of Tennessee, Knoxville, I agree that the Library shall make it available to borrowers under rules of the Library. Brief quotations from this thesis are allowable without special permission, provided that accurate acknowledgment of the source is made.

Permission for extensive quotation from or reproduction of this thesis may be granted by my major professor, or in his absence by the Head of Interlibrary Services when, in the opinion of either, the proposed use of the material is for scholarly purposes. Any copying or use of the material in this thesis for financial gain shall not be allowed without my written permission.

Signature ____________________

Date 26 Apr 91

DETERMINATION OF REENTRY PARAMETERS DURING

DESCENT FROM LOW EARTH ORBIT

A Thesis

Presented for the

Master of Science

Degree

The University of Tennessee, Knoxville

Steven W. Moss

August 1991

DEDICATION

This thesis is dedicated to my wife,

Sandra May Moss

who has given so much that I might achieve.

ACKNOWLEDGMENTS

I would like to thank my major professor, Dr. Firouz Shahrokhi, who has given me guidance and support. I would also like to thank the other committee members, Dr. Charles T. N. Paludan and Dr. Michael Chaney, for their comments and advice. I wish to express my sincere appreciation to Capt Ronald Stonum, USAF, who's forgotten more about computers than I ever knew, and was able to bail me out when I began to flounder. I would especially like to thank Lt Col Michael DeLorenzo, USAF, who alternately threatened and encouraged, and who provided the environment which made this thesis possible. Lastly, I wish to express my undying gratitude to my family, Sandy, Benjamin, Jennifer Robyn, and Kimberly, for their support, patience, and understanding.

ABSTRACT

This research attempted to develop a useful, interactive computer program to predict the reentry parameters on a vehicle as it descends to Earth from low earth orbit.

Beginning with a spacecraft in stable orbit, it determines the burn necessary to embark upon the desired trajectory through the atmosphere. The reentry path is initially described by the altitude, velocity and flight path angle. A numerical integration routine is performed to step down through the altitude levels, recomputing new values each step. The g loading is also determined at each altitude.

To validate the program US Space Shuttle flight STS-4 flight data were analyzed and compared to predictions from the program. The software had to account for a lifting body, gravity gradients, and flight vehicle roll angles. The Earth was treated as a non-rotating sphere, and the shuttle a point mass.

The program predicted the flight velocity of the shuttle well. Limitations of the program occur as the vehicle skips, as it tries to maintain level flight, and as the velocity slows too much. At shallow reentry angles the parameters were found to be very sensitive to small changes.

TABLE OF CONTENTS

LIST OF FIGURES

FIGURE PAGE

LIST OF SYMBOLS

a	Semi-major axis of orbit
B	Ballistic factor
C_D	Drag coefficient
C_L	Lift coefficient
E	Specific orbital energy
f	Error function
F	Force
F_a	Aerodynamic forces
F_g	Gravitational forces
FPA	Flight path angle
g	Gravitational acceleration
g_o	Gravitational acceleration at sea level
G	Universal Gravitational Constant
h	Specific angular momentum
H	Scale height
I	Inertial, Earth centered, reference frame
K	Lift to drag ratio
l	Vehicle reference frame alligned with gravity vector
m	Mass of reentry vehicle
m	Vehicle centered reference frame alligned with flight path angle
M	Mass of the Earth
n	Magnitude of the load vector, in sea level g's
n	Vehicle centered reference frame aligned with velocity vector

o	Vehicle centered frame alligned with vehicle bank angle
P	Linear momentum
p	Constant in temperature equation
q	Constant in temperature equation
r	Orbital radius from Earth's center
r_a	Radius of orbit at apogee
r_E	Radius of orbit at entry point
r_p	Radius of orbit at perigee
R_E	Radius of the Earth
s	Arc length, path through the atmosphere
S	Reference area
T	Static temperature of the atmosphere
v	Orbital velocity
V	Velocity during reentry
w	Cosine of the flight path angle
z	Altitude above the Earth's surface
α	Angle of velocity vector out of orbit plane
β	Ballistic coefficient
γ	Flight path angle
Ω_{IN}	Velocity vector rotations from inertial reference frame
ϕ	Bank angle
ρ	Density of the atmosphere
ρ_o	Reference density
λ	Nondimensionalized velocity squared
θ	Angle of orbit

CHAPTER 1

INTRODUCTION

The purpose of this thesis is to develop a computer model to predict the flight parameters of a reentry vehicle as it descends through the Earth's atmosphere. The main parameter of interest is the loading. Beginning with known entry conditions, the program will predict the loads on the reentry vehicle as it steps down through the altitude intervals.

There is rising interest in the use of space for commercial purposes, and of the many areas of interest is the recovery of small experiments from low earth orbit. The Center for Aerospace Propulsion (a joint undertaking by the University of Tennessee Space Institute and Calspan Corporation, Tullahoma, Tennessee) has been chartered by the National Aeronautics and Space Administration to develop the capability to return a life science experiment from the microgravity environment of space to the Earth's surface without damaging the experimental package. This has been translated into the requirement of not exceeding four times the gravitational acceleration at the Earth's surface any time during the reentry or impact.

The reentry package which detaches from the main satellite is called Freeflyer. The goal for industry is to develop this freeflyer concept into an integrated flight vehicle of booster and payload.

As private industry strives to meet this challenge, its proposals must be validated. This computer program will predict the loads on the Freeflyer reentry vehicle as it descends from low earth orbit. Beginning with the satellite in orbit the program will compute the velocity change necessary to deorbit the vehicle according to the desired initial flight path angle and altitude. The aerodynamic forces will be determined based upon lift and drag input data, which is assumed to be correct. The routine will perform a numerical integration, stepping down each altitude increment. The parameters solved for are the velocity, flight path angle, and the loading.

This program can become one of the tools used to analyze those proposals. It is intended to be an interactive Personal Computer based program. It will allow a fair degree of input modifications, so many different cases may be run in a short time. The output files are designed to be transferable into a spreadsheet, such as Lotus 123 Release 3, for pictorial interpretation of the results.

The programing language is Fortran 77 and was written for the Microsoft Fortran Compiler software. The Personal Computer used was a Unisys Personal Workstation Series 800/16.

The thesis will first trace the development of the gravity function and the density function, both of which vary with altitude and are inputs to the program. Next, the astrodynamic and aerodynamic equations of motion are developed and the numerical integration technique described. The program is then described, along with the associated input and output files and subroutines. The accuracy of the routine is validated against actual flight data from a U. S. Space

Shuttle mission. Finally, a few predictions involving a Freeflyer type vehicle will be demonstrated.

CHAPTER 2

EQUATIONS

REENTRY TRAJECTORIES

The reentry problem is one of using the aerodynamic drag of the Earth's atmosphere to provide a braking force as the reentry body travels through the air. By looking first at some very simple averages, the types of solutions needed will become clearer.

Assume first the maximum allowable deceleration can somehow be applied uniformly to the reentry vehicle during its entire flight profile. This would be "maximum" deceleration applied over the entire path length, and hence would indicate the most direct path through the atmosphere. For the following discussion a flat Earth is assumed.

First, the average acceleration is the change in velocity divided by the time, and the average velocity is the distance traveled divided by the time:

$$V_f - V_i = at$$

$$s_f - s_i = Vt$$

For the case of reentry and landing, the initial velocity is the entry velocity and the final velocity is zero. The final minus the initial position is the distance traveled. The average velocity is:

$$V = (V_f + V_i)/2 = V_E/2$$

Solving for time:

$$V_E = -at \quad or \quad t = -V_E/a$$

Solving for the distance:

$$s = (V_E/2)(-V_E/a) = -(V_E)^2/2a$$

What is the deceleration the atmosphere must to bring the vehicle to stop at the surface assuming a reentry normal to the Earth's surface Here it is assumed the atmosphere begins at 80 nautical miles. A typical reentry velocity is 25,000 ft/s.

$$a = -(V_E)^2/2s = -642.89\, ft/s^2$$

$$n = a/g = -\ 20\, g's$$

A vehicle reentering normal to the atmosphere will experience as a minimum, a maximum g loading of 20. Should any part of the reentry path experience less than 20 g's, some other portion must be above 20 g's to deposit the vehicle at the surface of the Earth at zero velocity. As mentioned before, this loading is too high for the life sciences experiments. The problem can be approached in a slightly different manner: What total distance must the reentry vehicle travel at a constant deceleration of 3 g's to stop at the surface with zero velocity?

$$s = -(V_E)^2/2ng = 3{,}241{,}029\, ft$$

$$s = 533\, nm.$$

This is 6 2/3 times the thickness of the atmosphere. An angled approach is required. Using simple plane geometry with the flat Earth assumption the required angle is shown in Figure 1. A steady glide path may not exceed 8.6 degrees and still yield a path of at least 533 nautical miles through the atmosphere.

This shallow entry corridor cannot be supported in a ballistic reentry, whose flight path angle grows to nearly 90 degrees. Some type of force is necessary to counteract the vehicle's natural tendency to burrow down into the atmosphere. This force may be either thrust or lift.

The retrothrust option is not likely. The cost in additional weight would be too great. To return a vehicle with the same relatively gentle acceleration that brought it into space would require the same amount of fuel it took to launch it originally. Therefore the launch fuel would have to be increased to lift the additional reentry fuel load.

A lifting body generates lift by virtue of its aerodynamic shape. This lifting force can be used to support the more gentle glide angle, adding only the weight of the additional structure and control system to the vehicle. This would presumably be smaller than the fuel loads.

It has long been known lifting bodies have such a salutary effect. Ely (1)[1] states that lifting reentry vehicle configurations permit a much lower maximum deceleration than is possible with a blunt,

[1]Numbers in parentheses refer to similarly numbered references in the List of References.

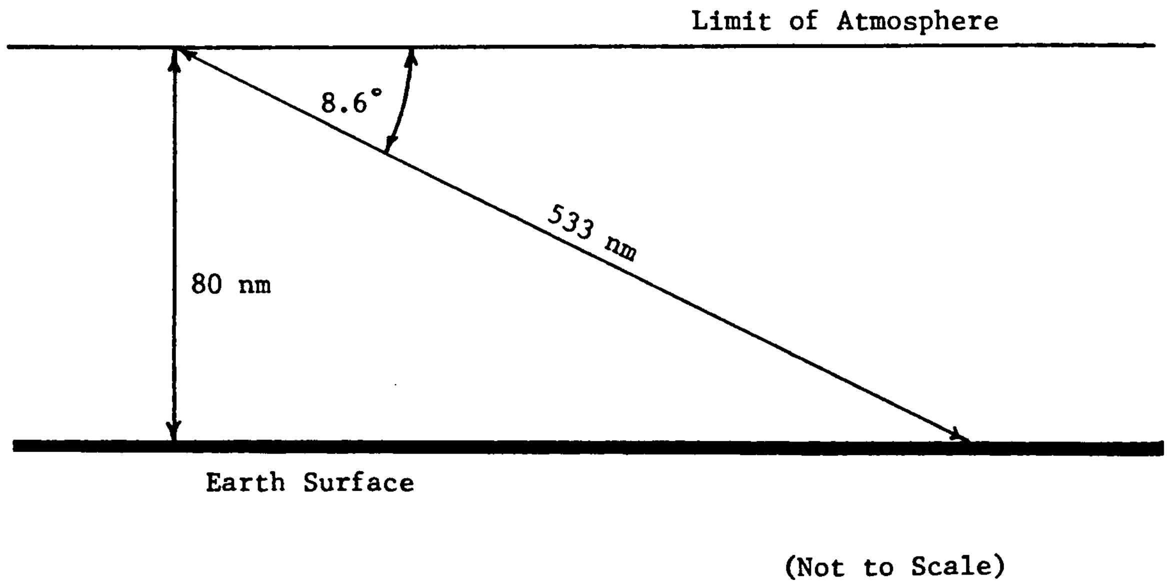

Figure 1. Constant G Flight Path Angle

ballistic missile reentry vehicle. Figure 2 shows the effect of lift to drag ratio on deceleration for entry into the Earth's atmosphere from decaying orbits. Notice the diminishing returns for increasing the L/D ratio. Negative lift causes the upper curve to bite harder into the atmosphere and increases the deceleration.

For this thesis the aerodynamic force coefficients will be inputs. No attempt is made to derive them or validate the accuracy of those inputs. Such realities as real gas effects are assumed to be incorporated within the input, but the quality of the output will depend upon the quality of the input.

Woods (2) has noted the real gas dynamics effects on the performance of lifting entry bodies has been understood, but modeling the real gas environments on both windward and leeward three dimensional surfaces is difficult. Bray (3) underscores the size of the problem by declaring the space shuttle is in the grip of this phenomena from above 300,000 ft to below 200,000 ft. This breakdown of the real gas assumption reinforces the fact much of what goes on at high altitude is not very well understood, and the likelihood of input error is great. Remembering that the lift and drag data are assumed correct, the quality of the prediction is based upon the effort expended in obtaining good input data.

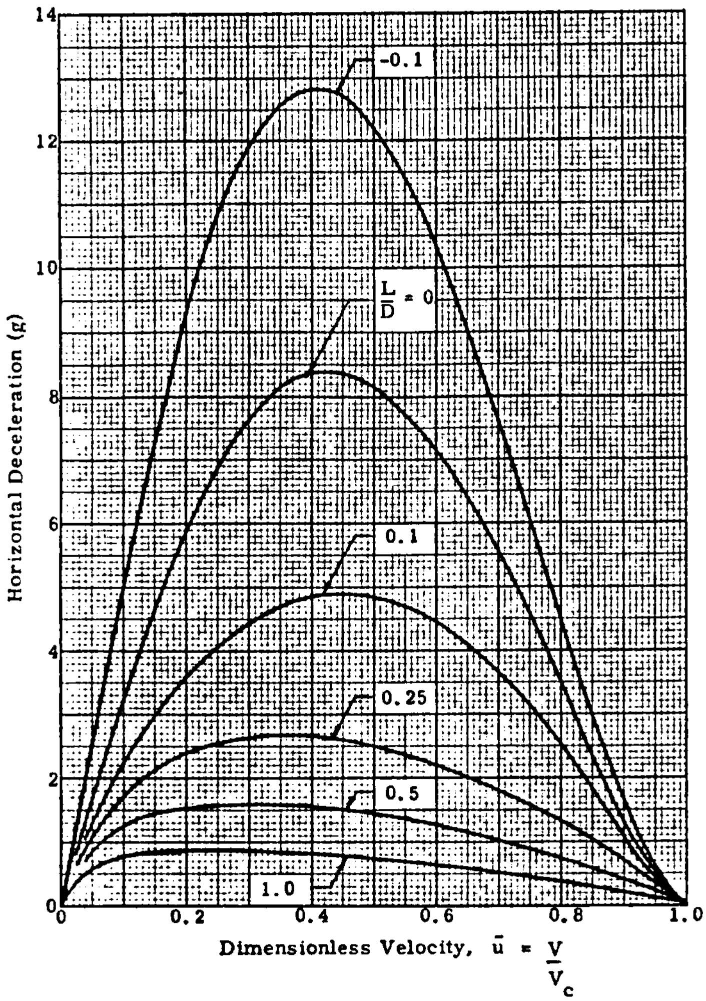

Figure 2. Load Variation with L/D

Source: Kork, Jyri, "Satellite Reentry," Design Guide to Orbital Flight, New York, NY: McGraw-Hill Books, 1962.

THE GRAVITY GRADIENT

The choice was whether or not to assume gravity is a constant. Regan (4) treats gravity as a constant, but Wiesel (5) chooses to incorporate a centripetal acceleration factor.

Here gravity will vary with altitude. The errors associated with a constant gravity would probably be small, but it is simple enough to use the gravity function:

$$F = GMm/r^2 = mg$$

where G is the Universal Gravitational Constant, M is the mass of the Earth, and r is the radius from the center of the Earth. The product $GM = 1.407647 \times 10^{16}\ ft^3/s^2$. At sea level, $r = R_E$, the radius of the Earth, 2.14112164×10^7 ft.

$$g_o = GM/(R_E)^2$$

In ratio with the gravity at altitude z:

$$g/g_o = (GM/(R_E + z)^2)/(GM/(R_E)^2)$$

or:

$$g = g_o\,(R_E)^2/(R_E + z)^2.$$

Here z is the altitude above the surface of the Earth such that $z=r-R_E$. The gravity at sea level, g_o, was taken to be $32.14824\ ft/s^2$ throughout.

MODELING THE ATMOSPHERE

By far the most complicated aspect was determining how to treat the atmosphere. The pressure and density vary too much to even consider treatment as constants. The question became how to best model the atmosphere.

There is no way to predict or solve for the actual atmospheric parameters. The changing weather is a testament to the great diversity and fluctuations nature is capable of. However, according to Dubin (6) some method of forming an atmospheric standard was necessary for scientists and engineers in the field to standardize flight vehicle instruments and flight vehicle performance.

The parameter of the atmosphere with greatest interest to reentry dynamicists is the density. This is because lift and drag are functions of density, related through the dynamic pressure.

$$L = \frac{C_L \rho V^2 S}{2} \; and \; D = \frac{C_D \rho V^2 S}{2}$$

are the well known relationships for lift and drag. These forms will be used in this thesis throughout the entire altitude range.

The most common model is the exponential used by Regan (4), Wiesel (5), and Hankey (7) to cite a few.

$$\rho = \rho_o e^{-z/H}$$

The ρ_0 term is a reference density that may or may not be equivalent to the density at sea level (depending upon whose model is being used). The denominator of the exponent is some scale height. Reagan's

(4) model uses (in English units) a reference density of .0034011 slug/ft^3 and a scale height of 21981.6 ft.

Figure 3 shows how this function compares with the 1962 U. S. Standard Atmosphere. This result was generated by writing a program to read from a density table, and to compute the density at that altitude by the Regan's (4) exponential formula. As can be seen, the error is slight but appreciable near sea level, and is minimal through 180,000 ft. Here the two predictions differ, but remain close until 420,000 ft where they diverge.

It is important to keep in mind the standard atmosphere is also a model and is not "real". The fact the exponential equation compares well with the tables does not mean it is correct at any particular time. Dubin (6) cautions that the 1962 US Standard Atmosphere is defined in terms of an ideal air assumed to be devoid of moisture, water vapor, and dust, and obeying the perfect gas law. During an actual descent local weather, winds aloft, humidity, or temperature may vary over a wide range. Table 1 from Craig (8) gives measured densities from 80 to 220 km (260,000 to 720,000 ft). A wide dispersion of densities are recorded from rocket data. The letter at the top corresponds to a different location and time that each of these measurements were taken. The extreme right column was data from the International Reference Atmosphere of the Committee on Space Research, and was used to curve fit a density function above 360,000 ft.

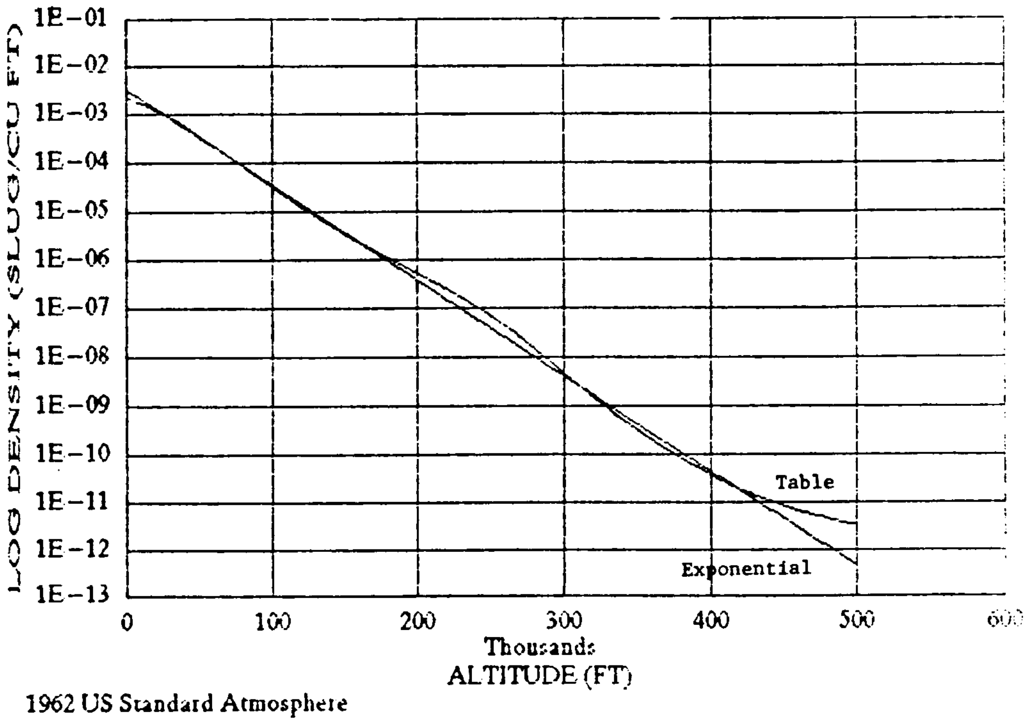

Figure 3. Exponential Density versus 1962 U. S. Standard

Table 1. Densities in the Thermosphere from Rocket Measurements

(A Partial Reproduction)

Alt (km)	Density (gm/cm-3)			
	A	B	F	L
100	2.5(10)	7.2(10)	-	4.8(10)
110	5.0(11)	1.3(10)	1.0(10)	9.5(11)
120	1.2(11)	2.6(11)	3.0(11)	2.4(11)
130	3.3(12)	6.4(12)	6(12)	7.0(12)
140	1.2(12)	3.0(12)	1.4(12)	3.1(12)
150	6.6(13)	1.9(12)	5(13)	1.7(12)
160	4.3(13)	1.4(12)	1.9(13)	1.1(12)

Parentheses gives negative power of 10

Key: A: 7 August 1951, White Sands, NM

B: 29 July 1957, Ft Churchill, Canada

F: 20 November 1956, Ft Churchill, Canada

L: International Reference Atmosphere

Source: Craig, Richard A., The Upper Atmosphere, New York, NY: Academic Press, 1965.

Craig (8) reports that differences by a factor as large as three exist. He states some may be from experimental error, but it is clear there is still a fair amount of variability. Dubin (9) also discusses density variations from standard in the 1966 Supplement to the 1962 US Standard Atmosphere. At altitudes around 230,000 ft the densities can vary as much as 20 percent. Groves (10) reports a seasonal variation of 40 percent. These are less than Craig (8) postulated, but the trend and the relative size of the departures are significant. Changes in the density can have a large effect on the reentry profile.

Despite the large uncertainties, which could cause significant deviations, some model must obviously be used. For greater accuracy at the higher altitudes the 1962 U. S. Standard Atmosphere was chosen over the exponential model. To implement this decision a choice had to be made between inputing a table to be read, or developing an equation. Using a table would greatly slow the the processing time of the program; therefore, an equation was developed.

The complete derivation of the density equation is offered in Appendix A. The initial assumption was that the atmosphere is a perfect gas:

$$P = \rho R T$$

The second assumption was that the hydrostatic equation applies:

$$dP/dz = -\rho g$$

Substituting the perfect gas law the base equation is obtained:

$$d(\rho RT)/dz = -\rho g$$

Unfortunately, density, temperature, and the gas constant R, are all functions of altitude. Nature does lend a helping hand in two respects, though. First, the gas constant, which is the universal gas constant divided by the molecular weight of the atmosphere, is a constant up to 300,000 ft. Above this altitude the molecular weight of air begins to decrease as the species present assume a greater proportion of lighter molecules. Assuming R constant, especially over small intervals, is justified.

The temperature cannot be assumed constant. However, the second favor nature bestowed was the fact the temperature gradients are linear. Figure 4, from Dubin (6), shows the variation with altitude up to 90 km (295,000 ft). Over each zone the temperature can be expressed as a simple linear function:

$$T = p + qz$$

The gravity is also a function of altitude. The equation has already been derived and is used here in a slightly different form:

$$g = g_o(1/(1 + z/R_E))^2$$

or

$$g = g_o(1 + z/R_E)^{-2}.$$

The final unwieldy result is called the complex integration equation:

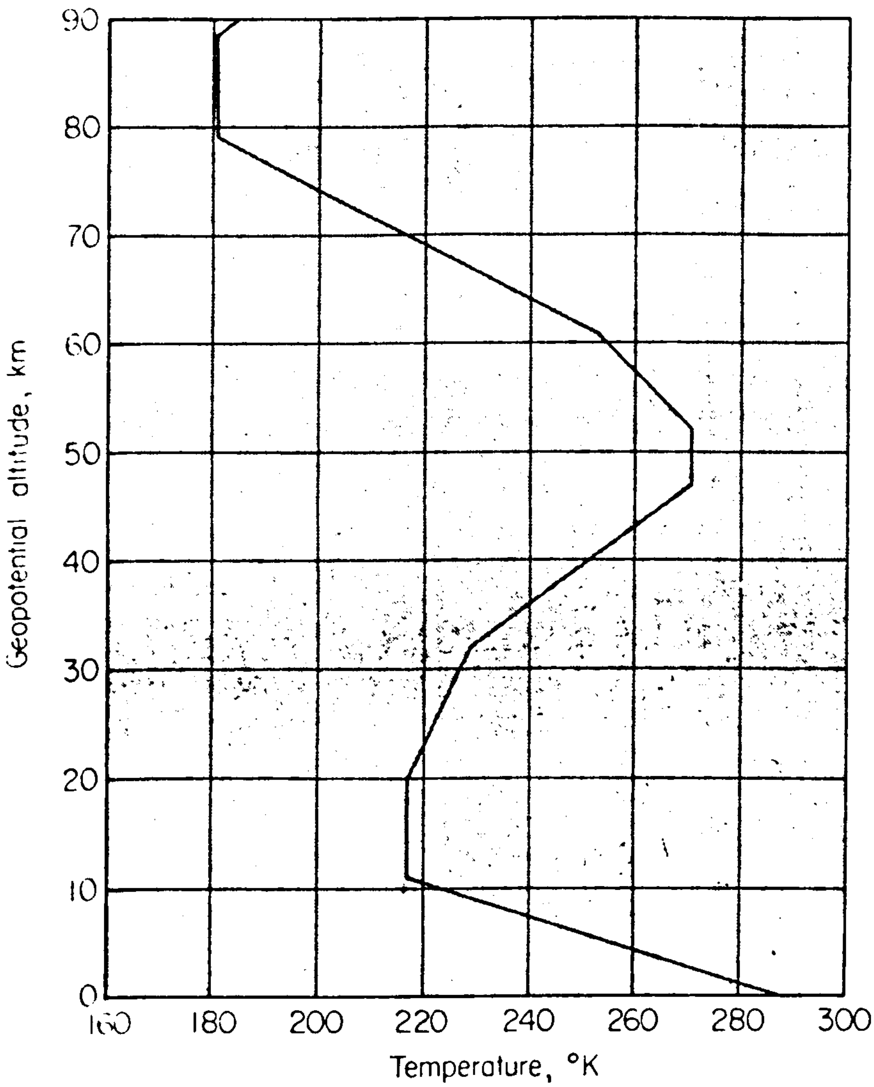

Figure 4. Temperature Variation with Altitude

Source: Dubin, Maurice, Editor, U. S. Standard Atmosphere, 1962, National Aeronautics and Space Administration, Washington, DC: U. S. Government Printing Office, 1962.

$$\rho_2 = \rho_1 \frac{p+qz_1}{p+qz_2} exp\{\frac{-g_o}{2R\left(q^2 - \frac{2qP}{R_E} + \frac{P^2}{R_E^2}\right)} \left[q\ell n \left[\frac{(p+qz_2)(1+z_1/R_E)}{(p+qz_1)(1+z_2/R_E)}\right]^2\right]$$

$$+ \frac{\left(q - \frac{2p}{R_E}\right)(z_1 - z_2)}{R_E(1+z_1/R_E)(1+z_2/R_E)}\Bigg]\}.$$

It still remains to solve for p, q, and ρ_1. The temperature constants, p and q, are solved by taking two points off the temperature line in each zone and deriving the equation for them.

Once the p and q have been determined the initial density is solved for. Starting at sea level and assuming the initial density to be 0.0023769 slug/ft^3, the density at the end of the zone is solved for. This final density becomes the initial density for the succeeding zone, due to continuity requirements. In this manner the p, q, and ρ_1 values for each temperature gradient zone are uniquely established.

These values are then read into a table. For a given altitude the values of p, q, and ρ_1 are selected and substituted into the equation. This process still requires a table, but searching through ten lines of zones is much quicker than searching through 450 lines of altitudes.

This technique worked very well to 360,000 ft. Above this altitude the temperature gradient is no longer linear. Trial and error was used and a curve fit was found that varied with altitude to the -2.7 power. Figure 5 shows the comparison between the curve fit and the

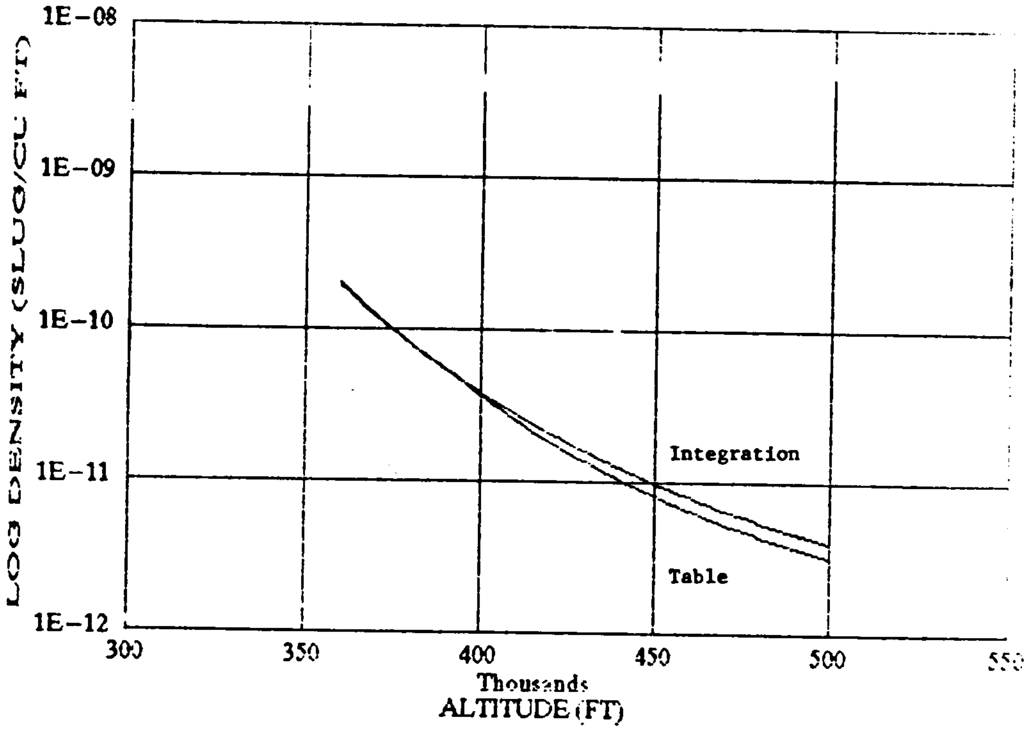

Figure 5. Density Curve Fit Above 360,000 ft

1962 U. S. Standard Atmosphere tabulated data. This was then spliced onto the end of the other equation. This combined curve is adequate through 500,000 ft.

Figure 6 shows the comparison between all three methods. Very good agreement is shown between the tabulated data and the complex integration equation. Figure 7 shows the percent log variation between the exponential equation and the tabulated data, and Figure 8 shows the variation between the complex integration data and the tabulated data. The exponential tracks fairly well to 200,000 ft, being around plus or minus 25 percent. Between 200,000 and 280,000 ft there is a large excursion to 80 percent variation. It again tracks well to 425,000 ft then diverges rapidly to 600 percent variation at 500,000 ft.

The complex integration data tracks exceptionally well throughout the entire range to 500,000 ft. It isn't until the altitude goes above 400,000 ft that the variation climbs above plus or minus seven percent. Even at its peak, the variation remains well below 25 percent.

Again, caution is advised in relying too strongly on these density numbers. The large fluctuations that may occur in the real atmosphere render the accuracy of the complex integration equation of less value. It is, however, an adequate rough-cut estimate of the density.

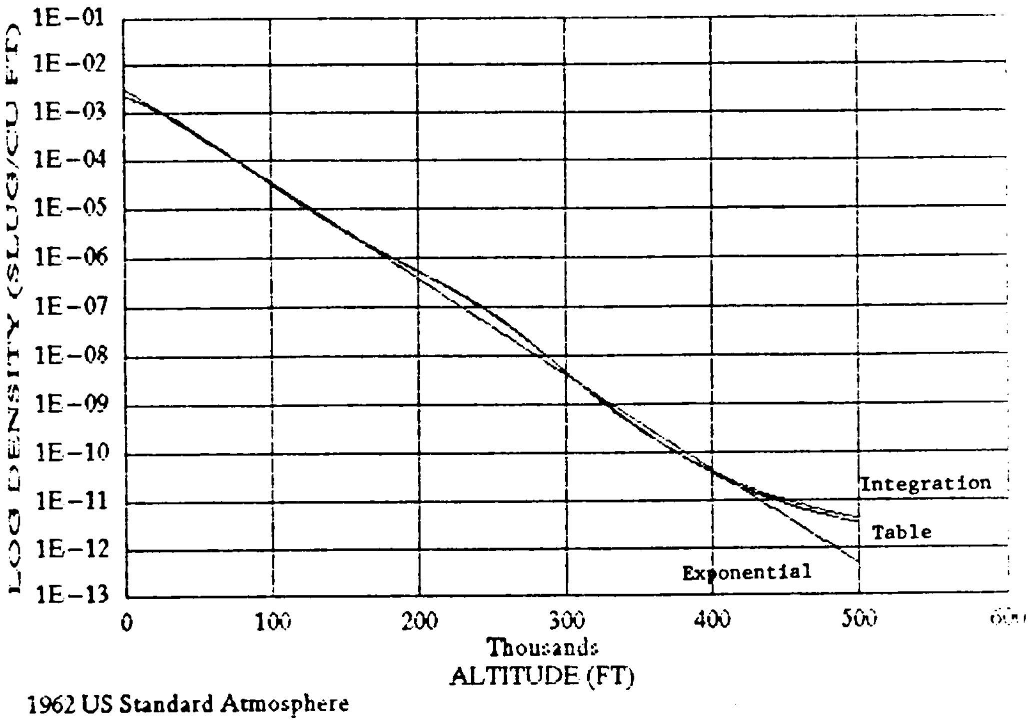

Figure 6. Comparison of Density Models to Standard

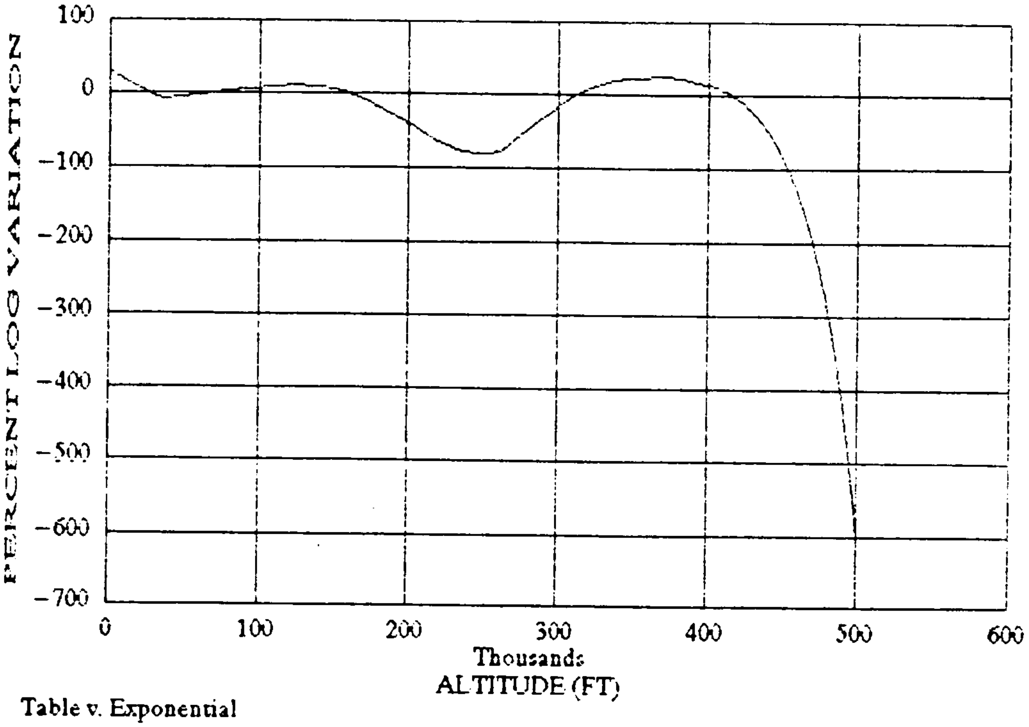

Figure 7. Difference Between Exponential and Standard

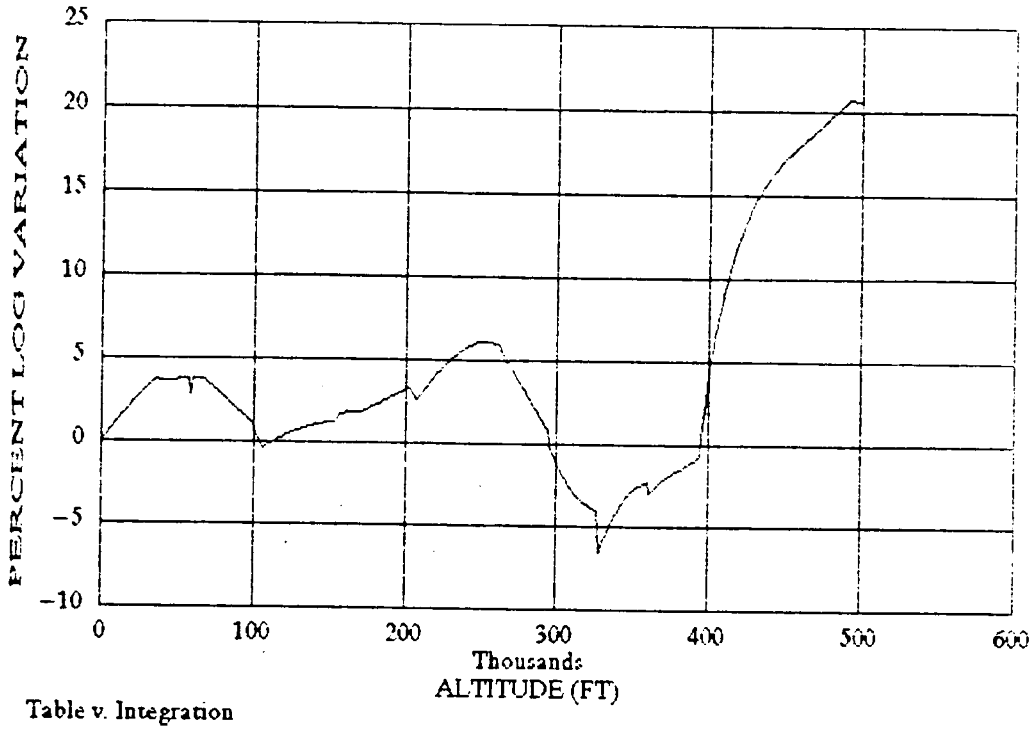

Figure 8. Difference Between Integrated and Standard

ORBITAL MECHANICS

This reentry problem begins with the vehicle orbiting the Earth. Rather than beginning at the reentry point, the starting point is a stable, low earth orbit. The problem now becomes one of how to deorbit the vehicle and place it into the reentry trajectory. Two different sets of equations govern the regimes of orbital flight and reentry dynamics.

The first task is to determine where this equation transfer should take place. At what altitude should the velocity and flight path angle be established to transition from the orbital, or Keplerian, to the aerodynamic equations.

A couple of sources were found to address this issue: Ehricke (11), and Duncan (12). Ehricke states the exact altitude of entry depends on many factors such as speed, shape, and to a lesser extent flight path angle.

Duncan goes much further by quantifying it. He first divides the trajectory into Keplerian, intermediate, and gas dynamic phases. The Keplerian phase is the orbital flight regime where the density is low and the gas dynamic forces are insignificant. The gas dynamic phase develops aerodynamic forces much greater than the gravitational forces. The intermediate phase has the two forces of comparable magnitudes.

Next, Duncan develops the concept of the conservation parameter, a name chosen for the quantity's close relation to the conservation of energy and angular momentum. He uncovered a complex relationship from which he determines where the Keplerian equations of motion should give way to the intermediate equations.

Duncan's formula is dependent upon reacting to time rate of change parameters read by the vehicle as it transits the atmosphere, however, and is not readily geared to the density change prediction algorithms used in this program. Also, his determination that the Keplerian equations give way when the conservation parameter changes by 10% is some what arbitrary. For the sake of simplicity, a fixed entry altitude will be chosen by the program operator.

To begin then, an assumption of the reentry altitude is made. Most of the published tables in Kork (13), when listing an altitude, quote one between 300,000 and 400,000 ft. Tucker (14) assumes 400,000 ft. Romere (15) considered the Shuttle to reenter at 350,000 ft. This seems to be a good estimate of the altitude, and it may not be necessary to go to Duncan's level of precision and complication.

Besides the altitude, the operator of the program is assumed to know another reentry input parameter, the flight path angle. The flight path angle is an important variable. This parameter has a pronounced effect on the loading. Ely (1) considers it very important in maximum load determination. The key to lifting body success in lowering the loading is in the ability to maintain low flight path angle flight. When running several simulations, the user will want to vary this quantity.

With the altitude and the flight path angle fixed, the velocity is uniquely determined, provided no additional forces act on the vehicle.

The program will determine the delta v required for a single burn at apogee to place the vehicle in the desired flight attitude at the proper altitude. (It will not take into consideration any specifically desired landing point.) However, an option exists for the program operator to input his own initial velocity.

One of the equations used in orbital mechanics stem from the relationships within the ellipse:

$$2a = r_a + r_p$$

which is a definition. The semi-major axis is one half the sum of the apogee plus perigee distance.

The energy equations result from the conservation of potential and kinetic energy. The potential energy arises from the gravitational potential, and the kinetic energy results from the motion of the body. Bate, et al. (16) states the specific mechanical energy is the mechanical energy per unit mass:

$$E = v^2/2 - GM/r$$

where G is the Universal Gravitational constant and M is the mass of the Earth, as denoted previously.

Another Bate, et al. (16) equation relates the energy to the orbital geometry:

$$E = -GM/2a$$

Rearranging:

$$E = -GM/(r_a + r_p)$$

Then combining:

$$-GM/(r_a + r_p) = v^2/2 - GM/r$$

$$v^2 = 2GM(1/r - 1/(r_a + r_p))$$

This equation yields the velocity magnitude at any point along the orbit as a function of the radius r. When r is the apogee, the velocity immediately prior to the deorbit burn is obtained.

The angular momentum of the spacecraft along the orbit is conserved and may be expressed:

$$h = rv\cos\gamma$$

When the position is either the apogee or perigee of the orbit, gamma equals zero and the equation reduces to:

$$h = rv$$

Working backwards, the flight path angle and the radius are knowns (they are the inputs). An expression for the velocity at entry using conservation of momentum is:

$$v_E = r_a v_a / r_E \cos\gamma$$

where E is the entry point, and a is the apogee.

A point should be made here about the burn at apogee. When burning either to slow down or speed up, the radius vector does not change at the burn location (assuming a burn parallel to the velocity vector). The velocity vector, and total angular momentum vectors change. Therefore, the new orbit has only the burn point in common with the old orbit. In other words, to effect a change at the reentry point the burn must occur elsewhere.

It is simplest to modify the apogee velocity for reentry. The perigee is closer to the Earth (by definition) and a small modification at apogee will lower the perigee further until it is well inside the atmosphere. To burn at perigee means the apogee point must be lowered until it is within the Earth's atmosphere. This is a much smaller orbit, and has much less angular momentum, therefore more change in the velocity vector is required than with the apogee burn.

After determining that the apogee burn yields the desired results, the entry strategy must be determined. One method would be to descend to perigee, which is now at the reentry altitude, burn again to change the vehicle flight path angle, and begin the reentry trajectory. A second method utilizes the natural flight path angle made by the elliptical shape of the orbit. By driving the desired flight path angle to occur naturally at the desired reentry altitude a single burn can accomplish the reentry insertion.

There are trade-offs between the two methods. The amount of burn at apogee required by the second method is greater than the first. This is because the perigee is lower than the first. The second burn, of course is avoided. A benefit of the second method, is it guarantees at the point defined as the reentry point, the vehicle will continue to descend without additional burning. Since it is a simpler method, it was chosen for the program.

The inputs to the program are: the orbit, defined by apogee and perigee altitudes, the desired reentry flight path angle, and the assumed reentry radius. It has already been demonstrated the orbital velocity at apogee can be solved for, as well as the velocity at the reentry point. What remains to be solved for is the velocity at apogee after the reentry burn. When this is determined the burn or delta v is known, which is the delta v required for a reentry trajectory at apogee. This leads ultimately to an equation which shows the effect a change in the entry flight path angle has on the burn required to initiate it.

Returning to the energy conservation equation the total energy at entry must equal the total energy immediately after reentry burn:

$$E = (v_E)^2/2 - GM/r_E = (v_a)^2 - GM/r_a$$

or,

$$(v_E)^2 - (v_a)^2 = 2GM(1/r_E - 1/r_a)$$

Replacing with the expression for v_E from above:

$$(r_a v_a / r_E \cos\gamma)^2 - (v_a)^2 = 2GM(1/r_E - 1/r_a)$$

$$(v_a)^2((r_a)^2/(r_E \cos\gamma)^2 - 1) = 2GM(1/r_E - 1/r_a)$$

Finally:

$$(v_a)^2 = \frac{2GM(1/r_E - 1/r_a)}{((r_a)^2/(r_E \cos\gamma)^2 - 1)}$$

The delta v required is now the difference between the two calculated va 's.

The velocity may now be calculated from the angular momentum equation previously listed.

AERODYNAMIC EQUATIONS OF MOTION

The equations of motion through the atmosphere must be determined with respect to an intertial reference frame. The center of a non-rotating Earth will be the origin of the intertial reference frame. The work in this section borrows heavily from the work in Regan (4), which is itself borrowed from Loh (17).

Next the vehicle's motion must be described. The vehicle will circle the Earth, and move in an arc around the Earth described by the angle theta. The Earth centered inertial reference frame, I, is shown in Figures 9 and 10. Here the Z_I vector points from the Earth's center to the reentry point. The plane formed between it and the Y_I vector describe the orbital plane of motion of the decaying orbit. The X_I vector is perpendicular to the other two inertial vectors.

The 1 reference frame shown in Figures 9 and 10 is vehicle centered such that the z_1 vector points from the center of gravity (the vehicle is assumed to be a point mass) to the center of the Earth as the vehicle descends through the atmosphere. The vector x_1 is in the orbital plane of motion described by the internal reference frame. The remaining vector y_1 is parallel to the X_I vector. As the vehicle follows its curved path about the Earth the angle theta the angular distance traveled from the entry point.

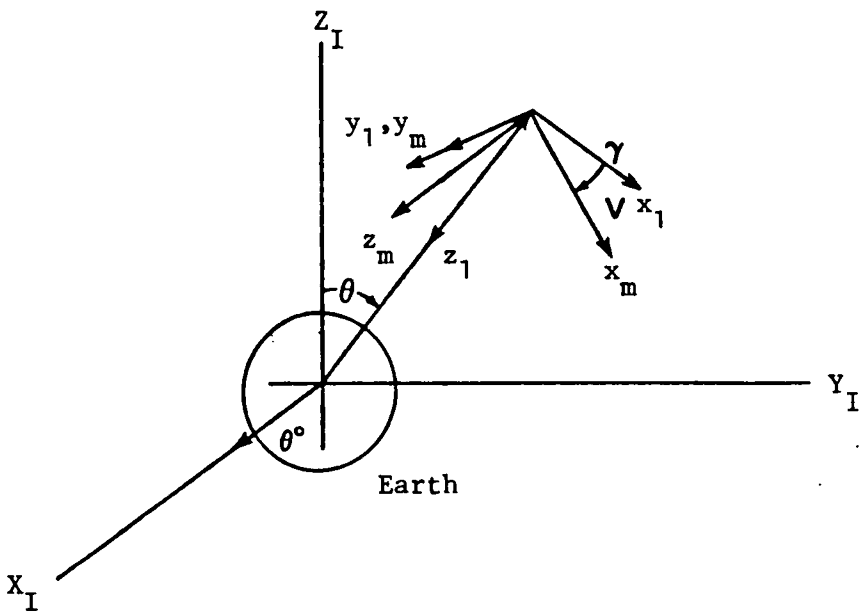

Figure 9. Inertial and Moving Reference Frames

Source: Regan, Frank J., Reentry Vehicle Dynamics, New York, NY: AIAA,, 1984

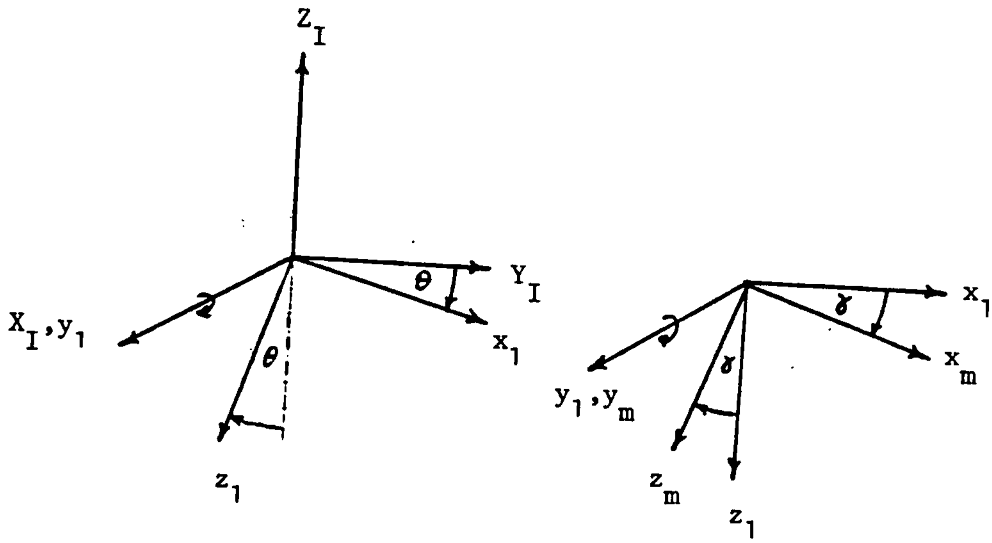

Figure 10. Reference frame Rotations in Orbit Plane

The m reference frame shown in Figures 9 and 10 is also vehicle centered, but the angular difference between the x_m and x_1 vectors is the flight path angle, gamma. The z_m vector is also in the orbital plane of motion, and the y_m vector is parallel to the y_1 vector.

Figure 11 shows the vehicle centered n reference frame. Here a bank angle causes a lift component to pull the vehicle out of the orbital plane of motion by the angle alpha. The x_n vector points in the vehicle's direction of motion, while the z_m and z_n vectors are parallel.

The final axis transformation occurs in the vehicle centered o reference frame and is detailed likewise in Figure 11. The z_o vector rolls by the angle psi from the z_n vector. The x_o vector is parallel to the x_n vector. The vectors involved are listed below:

$$\mathbf{V} = V x_n \qquad \Omega_{IM} = -(\dot{\theta} + \dot{\gamma}) y_I$$

$$\mathbf{L} = -L z_o \qquad \Omega_{MN} = \dot{\alpha}\, z_n$$

$$\mathbf{D} = -D x_n$$

$$\mathbf{g} = g z_1$$

All vectors are to be defined in terms of the n reference frame. Several coordinate transformations are required.

$$\begin{Bmatrix} x_m \\ y_m \\ z_m \end{Bmatrix} = \begin{bmatrix} \cos\gamma & 0 & \sin\gamma \\ 0 & 1 & 0 \\ -\sin\gamma & 0 & \cos\gamma \end{bmatrix} \begin{Bmatrix} x_1 \\ y_1 \\ z_1 \end{Bmatrix}$$

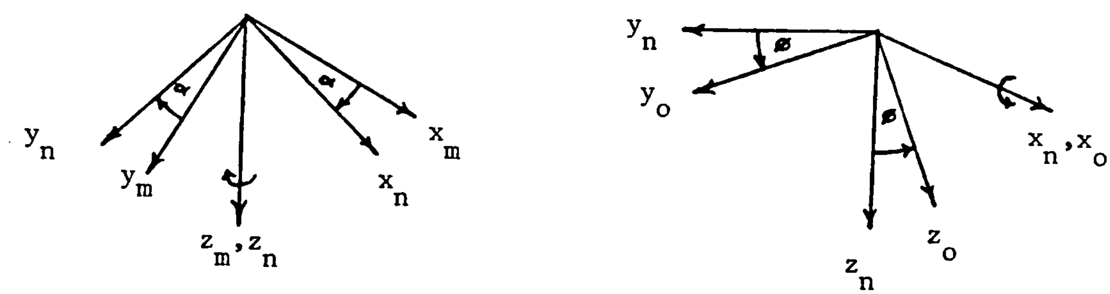

Figure 11. Reference Frame Rotations Due to Roll

$$\begin{Bmatrix} x_n \\ y_n \\ z_n \end{Bmatrix} = \begin{bmatrix} \cos\alpha & \sin\alpha & 0 \\ -\sin\alpha & \cos\alpha & 0 \\ 0 & 0 & 1 \end{bmatrix} \begin{Bmatrix} x_m \\ y_m \\ z_m \end{Bmatrix}$$

$$\begin{Bmatrix} x_n \\ y_n \\ z_n \end{Bmatrix} = \begin{bmatrix} 1 & 0 & 0 \\ 0 & \cos\phi & -\sin\phi \\ 0 & \sin\phi & \cos\phi \end{bmatrix} \begin{Bmatrix} x_o \\ y_o \\ z_o \end{Bmatrix}$$

Therefore, the vectors may be rewritten as:

$$\mathbf{g} = g\mathbf{z}_1 = g\,\sin\gamma\,\mathbf{x}_m + g\,\cos\gamma\,\mathbf{z}_m$$

$$= g\,\sin\gamma\,\cos\alpha\,\mathbf{x}_n - g\,\sin\gamma\,\sin\alpha\,\mathbf{y}_n + g\,\cos\gamma\,\mathbf{z}_n$$

$$\mathbf{L} = -L\mathbf{z}_o = L\sin\phi\mathbf{y}_n - L\cos\phi\mathbf{z}_n$$

$$\mathbf{D} = -D\mathbf{x}_n$$

$$\mathbf{V} = V\mathbf{x}_n$$

$$\Omega_{IM} = -(\dot{\theta} + \dot{\gamma})\mathbf{y}_m = -\sin\alpha\,(\dot{\theta} + \dot{\gamma})\mathbf{x}_n - \cos\alpha\,(\dot{\theta} + \dot{\gamma})\mathbf{y}_n$$

$$\Omega_{MN} = \dot{\alpha}\,\mathbf{z}_n$$

The acceleration of the vehicle is wanted. In an inertial reference frame this would be the derivative of the velocity vector. However, the vehicle motion has been described with respect to the n reference frame. Therefore:

$$a = dV/dt\,\mathbf{x}_n + \Omega_{IN}\, x\, \mathbf{V}$$

$$a = dV/dt\ \mathbf{x}_n - (\sin\alpha\,(\dot{\theta}\,\dot{} + \dot{\gamma})\mathbf{x}_n + \cos\alpha(\dot{\theta} + \dot{\gamma})\mathbf{y}_n - \dot{\alpha}\,\mathbf{z}_n)\, x\, \mathbf{V}$$

$$= dV/dt\ \mathbf{x}_n - (-V\cos\alpha\,(\dot{\theta} + \dot{\gamma})\,\mathbf{z}_n - V\dot{\alpha}\,\mathbf{y}_n)$$

$$= dV/dt\ \mathbf{x}_n + V\dot{\alpha}\mathbf{y}_n + V\cos\alpha\,(\dot{\theta} + \dot{\gamma})\,\mathbf{z}_n$$

The summation of the aerodynamic and gravity forces caused this net acceleration. Expressing them in force per unit mass, or acceleration:

$$\mathbf{F}_a/m = -D/m\,\mathbf{x}_n + L\sin\phi/m\,\mathbf{y}_n - L\cos\phi/m\,\mathbf{z}_n$$

$$\mathbf{F}_g/m = g\sin\gamma\cos\alpha\,\mathbf{x}_n - g\sin\gamma\sin\alpha\,\mathbf{y}_n + \cos\gamma\,\mathbf{z}_n$$

Equating the summed forces to the net acceleration caused, then listing by component the following result is obtained:

$$\mathbf{x}_n\!: g\sin\gamma\cos\alpha - D/m = dV/dt$$

$$\mathbf{y}_n\!: L\sin\phi/m - g\sin\gamma\sin\alpha = V\,d\alpha/dt$$

$$\mathbf{z}_n\!: g\cos\gamma - L\cos\phi/m = V\cos\alpha\,(\dot{\theta} + \dot{\gamma})$$

Lift and drag are now expressed in terms of their usual forms:

$$x_n\text{: } g \sin\gamma \cos\alpha - C_D \rho V^2 S/2m = dV/dt$$

$$y_n\text{: } C_L \rho V^2 S \sin\phi/2m - g \sin\gamma \sin\alpha = V\, d\alpha/dt$$

$$z_n\text{: } g \cos\gamma - C_L \rho V^2 S \cos\phi/2m = V \cos\alpha\,(\dot{\theta} + \dot{\gamma})$$

A new parameter is now introduced. The ballistic coefficient, beta, is described by Regan (4) as the "relative effect of the inertial force mg to the aerodynamic retarding force":

$$\beta = mg/C_D S$$

Other sources, such as Kork (13), use an alternate parameter B, the ballistic factor:

$$B = C_D S/2m = (g/2)/\beta$$

Beta will be used throughout. It has units of force per area.

$$x_n\text{: } g \sin\gamma \cos\alpha - g\rho V^2/2\beta = dV/dt$$

$$y_n\text{: } g\rho V^2 K \sin\phi/2\beta - g \sin\gamma \sin\alpha = V\, d\alpha/dt$$

$$z_n\text{: } g \cos\gamma - g\rho V^2 K \cos\phi/2\beta = V \cos\alpha\,(\dot{\theta} + \dot{\gamma})$$

where K = L/D and is the lift to drag ratio.

Some geometric relations are needed for some additional equations. Return to the coordinate transformations. It is desired to express the 1 reference frame in terms of the **n** reference frame:

$$\begin{Bmatrix} x_1 \\ y_1 \\ z_1 \end{Bmatrix} = \begin{bmatrix} \cos\gamma \cos\alpha & -\cos\gamma\sin\alpha & -\sin\gamma \\ \sin\alpha & \cos\alpha & 0 \\ \sin\gamma \cos\alpha & -\sin\gamma\sin\alpha & \cos\gamma \end{bmatrix} \begin{Bmatrix} x_n \\ y_n \\ z_n \end{Bmatrix}$$

$$x_1 = \cos\gamma \cos\alpha\, x_n - \cos\gamma \sin\alpha\, y_n - \sin\gamma\, z_n$$

$$y_1 = \sin\alpha\, x_n + \cos\alpha\, y_n$$

$$z_1 = \sin\gamma \cos\alpha\, x_n - \sin\gamma \sin\alpha\, y_n + \cos\gamma\, z_n$$

Differentiate and assume gamma and alpha are constant:

$$dx_1/dt = \cos\gamma \cos\alpha\, dx_n/dt - \cos\gamma \sin\alpha\, dy_n/dt - \sin\gamma\, dz_n/dt$$

$$dy_1/dt = \sin\alpha\, dx_n/dt + \cos\alpha\, dy_n/dt$$

$$dz_1/dt = \sin\gamma \cos\alpha\, dx_n/dt - \sin\gamma \sin\alpha\, dy_n/dt + \cos\gamma\, dz_n/dt$$

Motion, however, occurs only in the x_n direction, since $\mathbf{V} = Vx_n$. The y_n and z_n derivatives are zero.

$$dx_1/dt = \cos\gamma \cos\alpha\, dx_n/dt = \cos\gamma \cos\alpha\, \mathbf{V}$$

$$dy_1/dt = \sin\alpha\, dx_n/dt = \sin\alpha\, \mathbf{V}$$

$$dz_1/dt = \sin\gamma \cos\alpha\, dx_n/dt = \sin\gamma \cos\alpha\, \mathbf{V}$$

Also, looking at the 1 reference system:

$$dx_1/dt = (R_E+z)\, d\theta/dt$$

$$dy_1/dt = (R_E+z)\, d\alpha/dt$$

$$dz_1/dt = -dh/dt = -dz/dt$$

Here the scalar z is the altitude above the surface of the Earth. It can now be written:

$$dz/dt = -\sin\gamma \cos\alpha\, V$$

$$d\theta/dt = \cos\gamma \cos\alpha\, V/(R_E+z)$$

$$d\alpha/dt = \sin\alpha\, V/(R_E+z)$$

Differentiation with respect to altitude is preferred to differentiation with respect to time. The following mathematical rule will be helpful:

$$d(\,)/dt = d(\,)/dz\; dz/dt = -\sin\gamma \cos\alpha\; V\, d(\,)/dz$$

Substituting into the component equations:

$$x_n:\quad g \sin\gamma \cos\alpha - g\rho\, V^2/2\beta \;=\; -\sin\gamma \cos\alpha\, V\, dV/dz$$

$$y_n:\quad g\rho\, V^2 K \sin\phi/2\beta \;-\; g \sin\gamma \sin\alpha = V^2 \sin\alpha/(R_E+z)$$

$$z_n:\quad g \cos\gamma - g\rho\, V^2 K \cos\phi/2\beta \;-\; V^2\cos^2\alpha \cos\gamma/(R_E+z)$$

$$= -\sin\gamma \cos^2\alpha\, V^2\, d\gamma/dt$$

The three equations of motion may now be solved for. First, beginning with the x_n component:

$$V\, dV/dz = g\rho\, V^2/(2\beta \sin\gamma \cos\alpha) - g = 1/2\; d(V^2)/dz$$

$$d(V^2)/dz = g\rho\, V^2/(\beta \sin\gamma \cos\alpha) - 2g$$

Define $\lambda = V^2/R_E g_o$

$$\frac{d(V^2)H}{dz\, R_E g_o} = \frac{g\rho V^2 H}{R_E g_o \beta \sin\gamma \cos\alpha} - \frac{2gH}{R_E g_o}$$

$$\frac{d(\lambda)}{d(z/H)} = \frac{g\rho\lambda H}{\beta \sin\gamma \cos\alpha} - \frac{2gH}{R_E g_o}$$

It is now desired to convert the derivative with respect to altitude into a derivative with respect to density. The simplest expression for density is the exponential form:

$$\rho = \rho_o exp(-z/H)$$

whose derivative is

$$d\rho/d(z/H) = -\rho_o e(-z/H) = -\rho$$

However, the validity of using this approximation for density was earlier called into question. Assuming the 1962 U. S. Standard Atmosphere to be the "appropriate" density the differentiation should involve the complex integration formula. However, not only would the mathematics be difficult, but the resulting equation would be difficult to implement.

Perhaps the derivative of the exponential equation would be a sufficient approximation for the derivative of the complex integration equation. An error function can be developed to compare the derivatives of the two functions. If the error found is small enough, the derivative of the exponential function can serve as an accurate representation of the derivative of the complex integration density function.

$$difference = d\rho/dz_{int} - d\rho/dz_{exp}$$

To avoid having to differentiate the complex integration formula, use will be made of the simple limit function:

$$d\rho/dz = lim\, \Delta_{z \to o} (\rho(z + \Delta z) - \rho(z))/\Delta z$$

The error may now be defined:

$$error = f = difference/d\rho/dz_{exp}$$

forming the function:

$$d\rho/dz_{exp}(1 + f) = d\rho/dz_{exp} + difference$$

such that 1+f becomes the correction factor to equate the exponential derivative to the complex integration formula derivative.

After generating the error function, the values for f were between 10-6 and 10-8 for most of the range, except near the ends. Here the error was expected to be greatest since here the greatest divergence between the formulas developed. The error function here was on the order of 10-5. Figure 12 demonstrates this graphically. The curve was smoothed slightly to eliminate discontinuities. It seems clear the exponential function provides an adequate derivative function to the density equation. The following relation is then valid:

$$d(\lambda)/d(z/H) = d\rho/d(z/H)\, d(\lambda)d\rho = -\rho\, d(\lambda)d\rho$$

Returning to the x_n component equation:

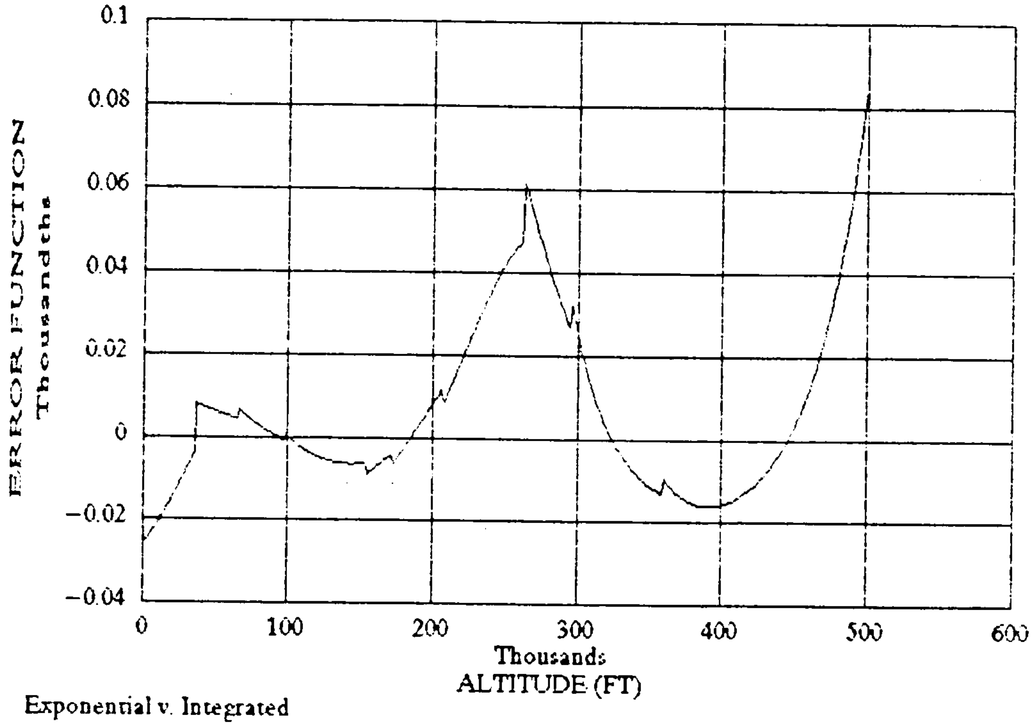

Figure 12. Density Derivative Error Function

$$-\rho\, d\lambda/d\rho = g\rho\, \lambda H/(\beta \sin\gamma \cos\alpha) - 2gH/R_E g_o$$

$$d\lambda/d\rho = 2gH/(R_E g_o \rho) - g\lambda H/(\beta \sin\gamma \cos\alpha) \qquad (1)$$

This is the final form of the velocity equation.

Now the y_n component equation is tackled. The alpha variable can be easily separated out:

$$V^2 \sin\alpha/(R_E+z) + g \sin\gamma \sin\alpha = g\rho\, V^2 K \sin\phi/2\beta$$

$$\sin\alpha\, ((V^2/(R_E+z) + g \sin\gamma) = g\rho V^2 K \sin\phi/2\beta$$

$$\sin\alpha = (g\rho V^2 K \sin\phi/2\beta)/(V^2/(R_E+z) + g \sin\gamma)$$

$$\alpha = \sin^{-1}((g\rho\, V^2 K \sin\phi/2\beta)/(V^2/(R_E+z) + g \sin\gamma)) \qquad (2)$$

An intuitive look at an expected reentry vehicle flight path questions the necessity of continuing to carry the α term. The ground track of such a vehicle would likely be very close to a straight line. The likelihood is that some other flight control input would be generated to keep the vehicle on more or less of a straight line, maneuvering rapidly in the alpha direction only at the lowest altitudes before touchdown.

The remaining variable is gamma. Beginning with the z_n component equation:

$$\sin\gamma d\gamma/dz = \cos\gamma/(R_E+z) + g\rho K \cos\phi/(2\beta \cos^2\alpha) - g \cos\gamma/(V \cos\alpha)^2$$

$$-d(\cos\gamma)/dz = \cos\gamma\,(1/R_E+z) - g/(V\cos\alpha)^2) + g\rho K\cos\phi/(2\beta\cos^2\alpha)$$

Define a new variable $w = \cos\gamma$.

$$-dw/dz = w(1/(R_E+z) - g/(V\cos\alpha)^2) + g\rho K\cos\phi/(2\beta\cos^2\alpha)$$

Using $\lambda = V^2/R_E g_o$

$$-dw/dz = w(1/(R_E+z) - g/(g_o R_E\lambda\cos^2\alpha)) + g\rho K\cos\phi/(2\beta\cos^2\alpha)$$

$$-dw/d(z/H) = wH(1/(R_E+z) - g/(g_o R_E\lambda\cos^2\alpha)) + g\rho HK\cos\phi/(2\beta\cos^2\alpha)$$

But $dw/d(z/H) = -\rho dw/d\rho$, therefore:

$$dw/d\rho = (wH/\rho)(1/(R_E+z) - R_E/(\lambda(R_E+z)^2\cos^2\alpha)) + gHK\cos\phi/(2\beta\cos^2\alpha)$$

$$dw/d\rho = (wH/\rho\,(R_E+z))\,(1 - R_E/(\lambda(R_E+z)\cos^2\alpha)) + gHK\cos\phi/(2\beta\cos^2\alpha) \qquad (3)$$

This is the final equation of aerodynamic force.

There are three equations and three unknowns: λ, α, and w. The solution for α is explicit. Unfortunately, λ and w are expressed in equations which are derivative forms of one another.

Since the equations cannot be solved analytically, they will be solved numerically. The equations are solved separately, first holding one variable constant and solving for the second variable, then solving for the first variable using the computed second variable as a constant.

The problem is an initial value one and according to Murphy, et al. (18) the Taylor's Series provides a good solution. The equations are of the form:

$$dx/dz = f(x,z), \quad x(z_o) = x_o$$

where x is either w or λ.

The Taylor's expansion is:

$$x(z_o + \Delta z) = x_o + (\Delta z/1!)x_o' + ((\Delta z)^2/2!)x_o'' + \ldots + ((\Delta z)^n/n!)x_o^{(n)}.$$

Appendix B provides the details of how this solution is carried out.

The final equation to derive is the loading equation. Here the loading is the acceleration the vehicle feels, divided by the acceleration due to gravity.

The accelerations have already been derived and equated to the aerodynamic and gravitational forces. The accelerations, by component are restated:

x_n: $dV/dt = g \sin \gamma \cos \alpha - C_D \rho V^2 S/2m$

y_n: $V \dot{\alpha} = C_L \rho V^2 S \sin \phi/2m - g \sin \gamma \sin \alpha$

z_n: $V \cos \alpha(\theta + \dot{\gamma}) = g \cos \gamma - C_L \rho V^2 S \cos \phi/2m$

The left hand side are the accelerations the vehicle feels. In dividing by the gravitational acceleration each load component is determined. The aerodynamic coefficients are also restated in terms of lift to drag ratio, and the ballistic coefficient. The load vector **n** becomes:

n_x: $\sin\gamma \cos\alpha - \rho V^2/2\beta$

n_y: $\rho V^2 K \sin\phi/2\beta - \sin\gamma \sin\alpha$

n_z: $\cos\gamma - \rho V^2 K \cos\phi/2\beta$

The solution to the magnitude of orthogonal vector components is to square each component, and take the square root of the sum:

$$n^2 = 1 + \rho^2 V^4 (1 + K^2)/4\beta^2 - (\rho V^2/\beta)(\sin\gamma \cos\alpha + \sin\gamma \sin\alpha\, K \sin\phi + \cos\gamma\, K \cos\phi).$$

The direction of the load vector is not of interest.

CHAPTER 3

THE PROGRAM

The program is actually a set of programs and data files. The programs are INPUT.FOR and REEN.FOR. The data files are LTD.DAT, ORBT.DAT, LOAD.DAT, and DEN.DAT. The first three must at least be established as files to start. The INPUT.FOR program generates the two of the three input files used by REEN.FOR. DEN.DAT is a file containing the density equation data used by REEN.FOR. The reason behind this two program system design is to be able to compile one reentry program and be able to vary the inputs without having to recompile after each run. The input program generates the input files and formats them. To run a modified entry condition it is necessary only to enter the input data files and make the required changes. If the modifications are major rerunning the input program might be best.

The program INPUT.FOR generates the files ORBT.DAT and LTD.DAT. ORBT.DAT is a file containing the orbital data. It contains the reentry altitude, apogee and perigee of the orbit, and the desired reentry flight path angle. There is an option to input a desired (forced) reentry velocity. If exercised this option assumes another burn to generate the required velocity without changing the orbital mechanics of the deorbit trajectory to that point. The file also contains information on the spacecraft's mass and reference area.

It continues with information controlling the numerical calculations by controlling the interval of the calculations as well as the altitude endpoint. This interval is important in that it needs to be small enough to let the solution converge. It is strongly recommended that an interval of 1000 ft be the maximum used. Finally, the program concludes by asking if the alpha should be ignored as a simplifying assumption.

Figure 13 shows an example of the ORBT.DAT file. The first entry is the reentry start in feet. The next two points are the apogee and perigee in nautical miles above the Earth's surface. Next comes the flight path angle in degrees followed by the forced velocity on/off flag and reentry velocity in feet per second. The mass in slugs is next, then the reference area in square feet, and finally, the interval and stopping point in feet, and the alpha on/off flag.

The file LTD.DAT containing the lift to drag tables used by the reentry program is shown in Figure 14. For each given altitude the table specifies the lift and drag coefficients, and the lift to drag ratio. Next to these column entries is the roll angle column. Most of the numbers here are nondimensional. The altitude is in feet, and the roll angle is in degrees.

The main program is REEN.FOR. It contains five subroutines and generates the output file LOAD.DAT containing the reentry parameters it calculates. The subroutines perform either calculations or table searches. The subroutine SCAN performs a table search of the LTD.DAT file, returning the lift, drag, and roll data appropriate for the altitude searched. If the altitude falls between table entries, the data from the higher altitude is selected.

```
350000.0000000
   171.0000001        171.0000000
     1.5000000
      .0000000           .0000000
  5435.0000000
  2690.0000000
   500.0000000
 10000.0000000
     1.0000000
```

Figure 13. ORBT.DAT Input File

265000.	.75	.72	1.04	.0
250000.	.75	.72	1.04	-74.0
247000.	.83	.76	1.09	-72.0
245000.	.81	.75	1.08	-73.0
243000.	.86	.78	1.10	-78.0
242000.	.80	.77	1.04	-78.0
240000.	.78	.78	1.00	-71.0
238000.	.76	.76	1.00	-68.0
237000.	.78	.75	1.04	-64.0
234000.	.82	.74	1.14	-63.0
232000.	.82	.75	1.09	-70.0
230000.	.83	.75	1.11	-70.0
229000.	.87	.84	1.04	-60.0
227000.	.88	.85	1.04	-60.0
225000.	.87	.84	1.04	-60.0
222000.	.87	.83	1.05	-60.0
220000.	.86	.82	1.05	-60.0
217000.	.86	.81	1.06	-60.0
214000.	.85	.80	1.06	-60.0
211000.	.85	.80	1.06	-60.0
209000.	.87	.82	1.06	-60.0
207000.	.88	.82	1.07	-63.0
203000.	.90	.84	1.07	-60.0
200000.	.90	.83	1.08	-60.0
197000.	.91	.84	1.08	-64.0
193000.	.93	.87	1.07	-66.0
189000.	.92	.87	1.06	-58.0
186000.	.91	.84	1.08	-52.0
182000.	1.00	1.06	.94	-58.0

Figure 14. LTD.DAT Input File

Subroutine DEN calculates the density at a given altitude. It performs a table search of the input file DEN.DAT, shown in Figure 15, which contains the p, q, $\rho 1$ and molecular weight constants for the density equations, then computes the density based upon those inputs. The subroutine DELT computes the difference in densities for the altitude interval under consideration. It calls upon DEN subroutine to compute the second density, then performs the subtraction. The densities and differences will be used in the numerical integrations to follow.

LAM and CGAM are the subroutines which perform the two numerical integrations. LAM assumes a constant flight path angle and computes the velocity change as the vehicle descends between two altitudes. Since the equations are written it terms of density the altitudes are converted into densities by the subroutines DEN and DELT. The Taylor expansion is carried out to seven terms to ensure the final increment is negligible compared to the first. The exponents became so large or small that double precision had to be used, due to its greater range. The difference is that single precision can accommodate exponents up to plus or minus 37, while the double precision can carry calculations out to plus or minus 307.

The equations listed in Appendix B are then computed and returned to the main program, where CGAM picks them up. CGAM assumes the velocity is constant and computes the change in flight path angle. The velocity used is an average value between the beginning and ending

328000.	-326.697	2.151515E-003	9.09481101E-010	28.88
295000.	-257.121	1.939394E-003	6.2410999E-009	28.96
262000.	315.	0.	4.216025E-008	28.96
207000.	958.091	-2.454545E-003	4.1810209E-007	28.96
172000.	674.743	-1.085714E-003	1.501661E-006	28.96
154000.	488.	0.	2.964053E-006	28.96
98000.	265.25	1.446428E-003	3.685933E-005	28.96
66000.	354.9375	5.3125E-004	1.75977E-004	28.96
36000.	390.	0.	7.37768E-004	28.96
0.	528.	-3.833333E-003	2.377E-003	28.96

Figure 15. DEN.DAT File

values to come out of LAM. CGAM requires the double precision for the same reasons LAM does.

At the end of the subroutine it is possible a negative flight path angle would result. This would result when the function attempts to return a value greater than one. The routine would then attempt to take the arccos of that value. This would cause the program to terminate in error.

To work around this limitation, it was assumed the axis could, in effect, be rotated 180 degrees about the horizon. It was assumed a value greater than one was an imaginary representation of a number equal to the identical amount less than one, but in the negative gamma direction. The subroutine computes this value as a negative flight path angle, and also returns a flag indication the vehicle is ascending. This flag then indicates to the main program the next altitude increment needs to be in the positive z direction, instead of stepping down in the negative direction.

A message is written to the screen the first time to indicate the vehicle has "skipped" in the atmosphere. It will not repeat the message for subsequent skips.

REEN.FOR begins by reading the values in the ORBT.DAT file. It then ensures the apogee is the greater altitude than the perigee, and, if not, it switches them. The orbital mechanics calculations occur next, culminating in the altitude, flight path angle, and velocity initial conditions for the aerodynamic equations. The initial apogee velocity, the apogee velocity after deorbit burn, the total delta v (including a second burn at reentry if that option is selected), and the velocity at the entry point are then written to the screen.

The next phase begins by calling upon DEN to compute the density at the entry altitude. The actual force of gravity is computed, and the velocity is nondimensionalized to the function lamda. The subroutine SCAN then selects the appropriate aerodynamic coefficients for that altitude. The next altitude is determined by the interval input and DELT calculates the density at that altitude and the difference between the densities.

The subroutine LAM then computes the new value for lamda, assuming a constant flight path angle. The average lamda is then determined for that interval and that value is collected by CGAM and the difference in flight path angle is determined assuming a constant average lamda.

At this point the loads on the vehicle are calculated. This load factor is tracked and the maximum load and altitude are written to the screen at the conclusion of the program. The computer also writes the altitude to the screen every 40,000 ft to reassure the operator the program is running.

This serves as an important check. Sometimes the altitude will increase continuously indicating the vehicle has skipped completely out of the atmosphere. The user can terminate the program (using control-C) and reconfigure the ORBT.DAT file to attempt another condition. This program works best with a continuing downward motion through the atmosphere. Small skips are believed to be reasonably predicted and worked through. Large skips, however, are not represented here as being accurately described. The intent of the thesis was to provide a low g prediction for reentry. The skipping reentry is not a low g return and is considered beyond the scope of this thesis.

Another blind spot of this program is the inability to tolerate flight at constant altitude. Were the vehicle to fly truly level there would be no stepping down or up in the integration scheme. The program will error terminate. The user should try to rerun the program using a different interval, as this sometime helps. If it does not some other flight parameter will need changing.

It remained to write the computed parameters into the output file LOAD.DAT. They are written without headings, as this facilitated the importation to the Lotus 123 spreadsheet for graphical representation. The final interval solutions are redefined as the initial inputs and the program returns to compute at the next altitude increment. This loop continues until the lowest altitude is reached, or an illegal calculation is attempted.

A portion of the LOAD.DAT file is reproduced in Figure 16. The first column contains the altitude, followed by g loading, velocity, and flight path angle columns. The next two columns are the lift to drag ratio, and the ballistic coefficient. The final column is the density.

The programs INPUT.FOR and REEN.FOR are reproduced in their entirety in Appendix C.

205500.	2.10	23142.	1.08	1.07	77.68	.441392E-06
205000.	2.14	23096.	1.04	1.07	77.68	.449843E-06
204500.	2.17	23048.	1.00	1.07	77.69	.458446E-06
204000.	2.20	22997.	.95	1.07	77.69	.467203E-06
203500.	2.23	22942.	.90	1.07	77.69	.476117E-06
203000.	2.27	22882.	.84	1.07	75.85	.485191E-06
202500.	2.31	22817.	.77	1.07	75.85	.494427E-06
202000.	2.33	22744.	.69	1.07	75.85	.503827E-06
201500.	2.36	22662.	.60	1.07	75.86	.513395E-06
201000.	2.39	22566.	.49	1.07	75.86	.523134E-06
200500.	2.41	22446.	.35	1.07	75.87	.533045E-06
200000.	2.40	22284.	.09	1.08	76.78	.543133E-06
199500.	2.31	21626.	-.33	1.08	76.79	.553400E-06
200000.	2.23	21450.	.46	1.08	76.78	.543133E-06
199500.	2.24	21328.	.33	1.08	76.79	.553400E-06
199000.	2.25	21157.	.08	1.08	76.79	.563848E-06
198500.	2.14	20411.	-.31	1.08	76.79	.574482E-06
199000.	2.06	20228.	.43	1.08	76.79	.563848E-06
198500.	2.07	20100.	.31	1.08	76.79	.574482E-06
198000.	2.08	19923.	.11	1.08	76.80	.585304E-06
197500.	2.01	19398.	-.27	1.08	76.80	.596317E-06
198000.	1.93	19192.	.39	1.08	76.80	.585304E-06
197500.	1.94	19052.	.28	1.08	76.80	.596317E-06
197000.	2.01	18853.	.17	1.08	75.89	.607524E-06

Figure 16. Sample of LOAD.DAT File

CHAPTER 4

VALIDATION

THE DATA

Considerable effort was expended in locating some reentry data. The type of reentry vehicle desired was a satellite or a space capsule like Gemini or Apollo, because this type of flight vehicle is anticipated to be more representative of the expected type of reentry satellites industry will propose. This data was not easily obtainable from the open literature. Only space shuttle data was easily found.

Data from the U. S. Space Shuttle was not the type of vehicle data this program was intended to predict. The shuttle is the most complicated flight vehicle ever built, performing many more flight activities than the simple ones serving as inputs for this program. However, it was the only flight data easily available.

Even then the format of the data was not good. The source of the data was NASA Conference Publication 2283 Part I, a shuttle performance lessons learned conference. The first order of business was to obtain the lift and drag data. This was gleaned from a graph in Compton (19) specifying the coefficients of lift and drag as a function of Mach number, reproduced here in Figure 17. The excursions at Mach 12 and Mach 8 were the result of intentional pull up maneuvers during the reentry to test the shuttle's control lability.

The program was designed to input aerodynamic coefficients as a function of altitude, not Mach number. Compton (19) provided another

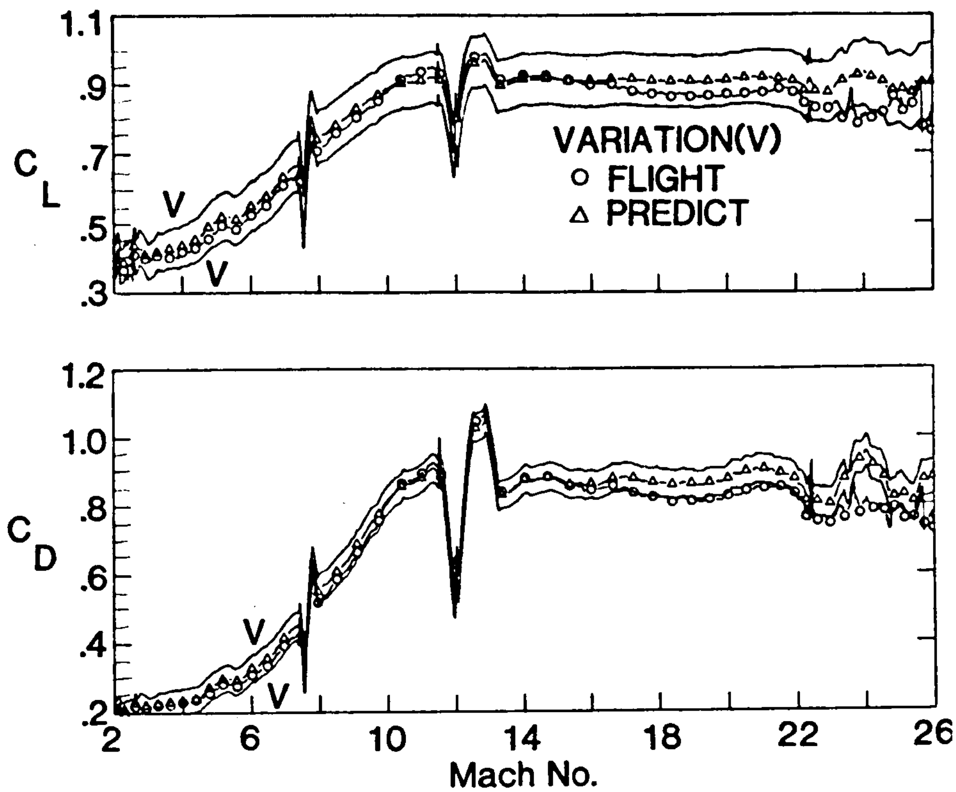

Figure 17. Lift and Drag Coefficients STS-4

Source: Compton, Harold R., Schiess, James R., Suit, William T., "Stability and Control Over the Supersonic and Hypersonic Speed Range", NASA Conference Publication 2283 Part I,Hampton, VA: NASA, 1983 graph demonstrating the relation between velocity and time, and altitude and time. By picking points off the two curves at the same time it was possible to develop a curve fitting routine to predict the velocity at a given altitude. The graph used is shown in Figure 18.

The missing element was provided in another paper by Romere (15), where Mach number and altitude were displayed. Another curve fit was developed to predict Mach number as a function of altitude. The data is shown in Figure 19 and the curve fit is shown in Figure 20 with some data points plotted along the curve.

It is now possible to develop the aerodynamic coefficients as a function of altitude. Using the curve in Figure 17, the lift and drag coefficients are taken as a function of Mach number. Using the generated curve in Figure 20 the altitude is then picked off for that event. This is how the table LTD.DAT was generated.

The output of the program was then compared against the velocity versus altitude curve fit generated from Figure 18. For purposes of validation another program FLV.FOR was written. This program reads down the LOAD.DAT table and for each altitude entry it computes a corresponding flight velocity value. In this way any skips which might result from the program automatically had an associated flight velocity. While this would not reflect an actual event, it does allow easier graphing by maintaining a one to one correspondence between altitude and velocity entries. The altitude, the reentry program generated velocity, and the flight data curve fit generated velocity

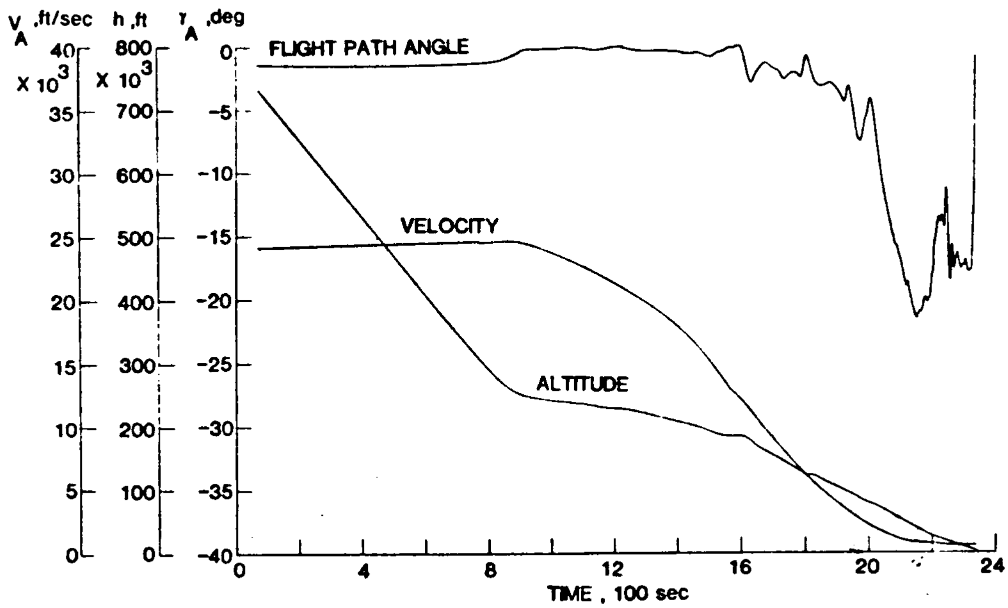

Figure 18. Velocity and Altitude Profiles STS-4

Source: Compton, Harold R., Schiess, James R., Suit, William T., "Stability and Control Over the Supersonic and Hypersonic Speed Range", NASA Conference publication 2283 Part I, Hampton, VA: NASA, 1983

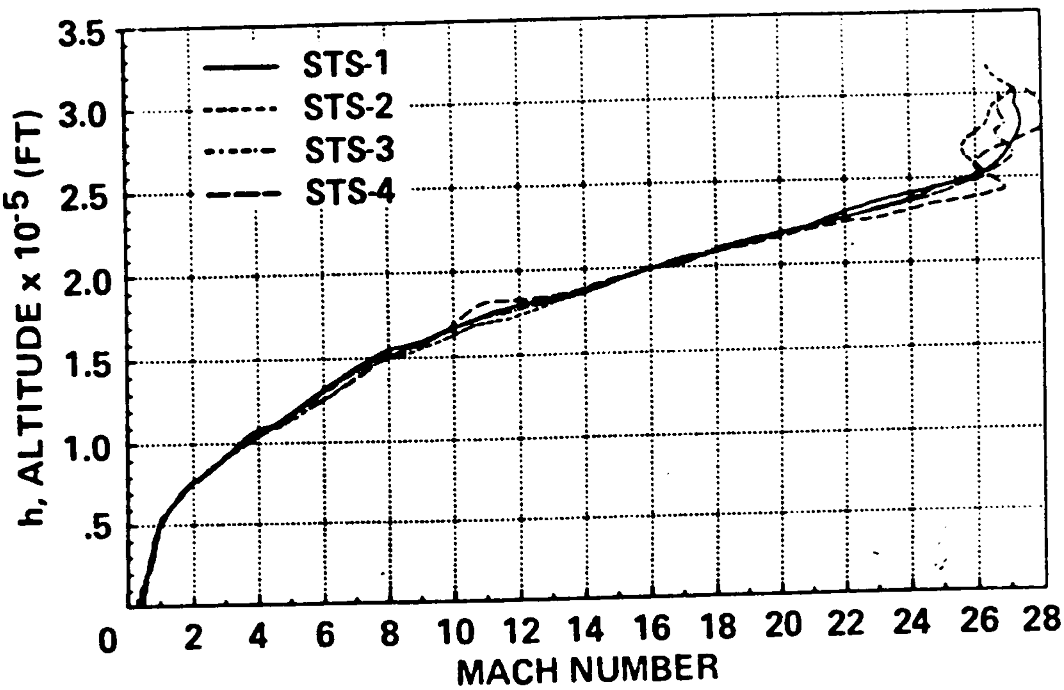

Figure 19. Altitude versus Mach Number STS-4

Source: Romere, Paul O., Whitnah, A. Miles, "Space Shuttle Entry Longitudinal Aerodynamic Comparisons of Flights 1-4 with Preflight Predictions", NASA Conference Publication 2283 Part I, Hampton, VA: NASA, 1983

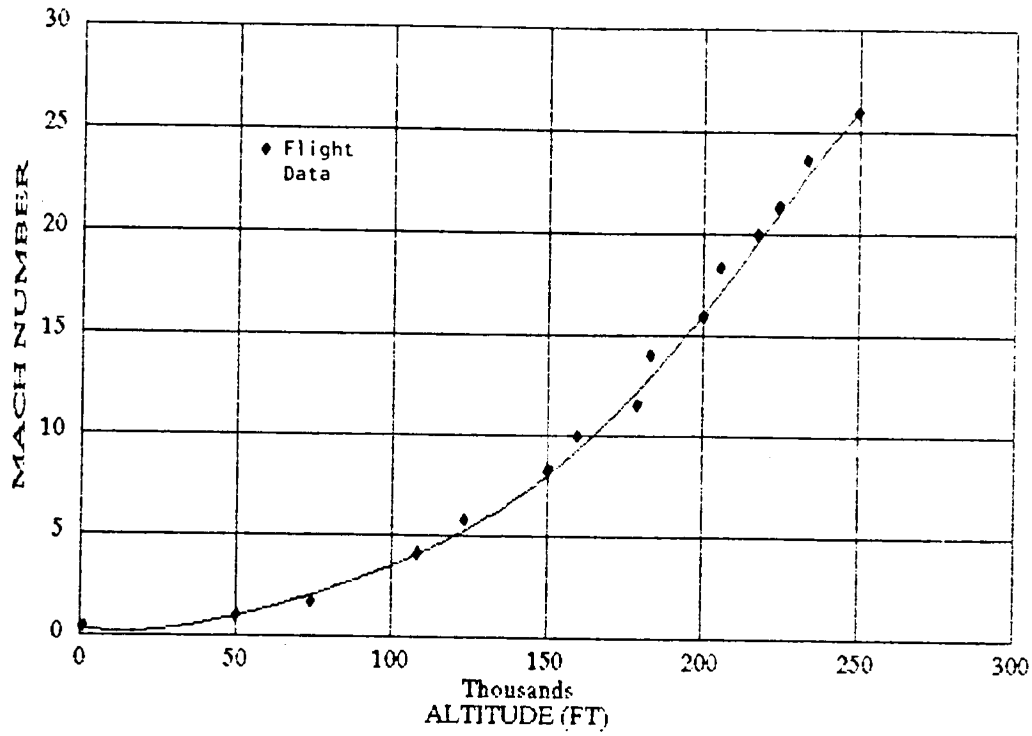

Figure 20. Mach Number versus Altitude Curve Fit

were all recorded in an output file called FLV.DAT. This file was then imported into a Lotus 123 spreadsheet for graphing.

The shuttle flight profile control program has the vehicle performing some roll to control range and cross track errors. In another graph Romere (15) displayed roll angle as a function of Mach number, shown in Figure 21. Again, using the Mach number and altitude graph the roll angle was entered into the LTD.DAT table as a function of altitude. This completes the LTD.DAT table.

Information is now required for the ORBT.DAT table. Figure 18 was used to determine the initial entry parameters. At an altitude of 350,000 ft, the velocity is 24,430 ft/s (from the curve fit equation), and the flight path angle is 1.5 degrees. From a summary of space orbital data by Thompson (20), shuttle flight STS-4 was on a circular orbit at 318 km. This corresponds to an altitude of 171 nautical miles. The reference area is the wing area, 2690 ft^2. The mass comes from a 165,000 lbf empty weight according to Joels (21), which was assumed to be 175,000 lbf when loaded, returning to Earth. This translates to 5435 slugs, mass. The lower limit was set to 10,000 ft and the interval was set to 500 ft. No velocity modification was anticipated. That completed the ORBT.DAT table.

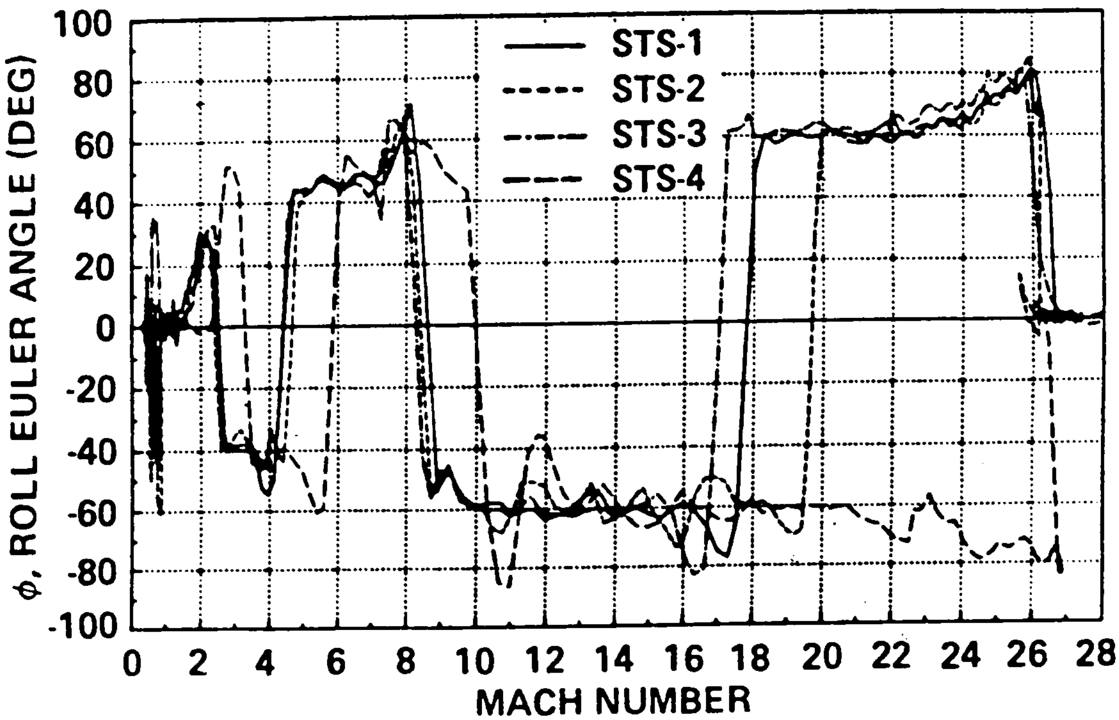

Figure 21. Roll Angle STS-4

Source: Romere, Paul O., Whitnah, A. Miles, "Space Shuttle Entry Longitudinal Aerodynamic Comparisons of Flights 1-4 with Preflight Predictions", NASA Conference Publication 2283 Part I, Hampton, VA: NASA, 1983

EXECUTING THE PROGRAM

In running the program a problem was immediately encountered with the alpha equation. At 250,000 ft the prediction was the shuttle would be turned by 90 degrees. This did not happen in flight. Bennet (22) discusses the shuttle entry flight control profile. The bank maneuvers conducted occur about the velocity vector, rather than the vehicle centerline. This is because the vehicle must maintain an orientation to prevent side heating. The vehicle control is maintained by a combination of the reaction control system and the aerodynamic control surfaces.

The program has no counterforce mechanism other than to assume the shuttle would fly in a reasonably straight line and shut the alpha equation down. The ORBT.DAT table was entered, and the alpha flag was changed from 0 to 1. The program was restarted.

Figure 22 shows the screen messages generated by the program execution. The first line shows the velocity at apogee before burnout, 25,316 ft/s, and immediately after deorbit burn, 24975 ft/s. The delta v is -341 ft/s, indicating the vehicle must slow by this amount. The V entry is the velocity at the entry point. Since the radius is shorter at the entry point, the velocity must be larger to conserve angular momentum. The next set of entries show the program steadily stepping down through the altitude intervals. Somewhere between 270,000 ft and 231,000 ft, the vehicle is forecast to experience a skip. Others may occur during the descent, but only the first one is annotated on the screen.

```
TED 1.0 (c) 1988 Ziff Communications Co.
PC Magazine ~ Tom Kihlken
C:\FORTRAN\TEMP>reen
 VA=   25316.   VAB=   24975.   DV=    -341.   V=   25793.
       310000.
       270000.
SKIP!
       231000.
       191000.
       152000.
       112000.
        73000.
        33000.
? Error: ARCSIN or ARCCOS of REAL > 1.0
  Error Code 2132
PC = 1C99: 00AF; SS = 216D, FP = E9BA, SP = E9BC


C:\FORTRAN\TEMP>
```

Figure 22. Screen Display STS-4 Prediction

The program ran this time until it had reached an altitude between 33,000 ft and the termination altitude. It stopped and an error message indicates an attempt to take an inverse trigonometric function illegally. This was the flight path angle going divergent. Experience with the program shows very erratic behavior when the velocities fall below 500 ft/s. However, by calculating the parameters to below 33,000 ft, enough data is obtained to make a comparison with flight data.

Figure 23 shows the comparison of the flight velocity data to the predicted velocity data. Initially, the simple deorbit maneuver has the vehicle entering the reentry trajectory at 25,793 ft/s instead of the 24,431 ft/s given by the flight data. This amounts to a 5.6% error. The relatively small error justifies the use of the simple deorbit model.

As the atmosphere begins to brake the vehicle the velocities begin to track much better. Ironically, the flight data is the smoother curve, compared to the predictions. There is a slight flaw in the smoothness where two equations splice together at about 180,000 ft. The prediction tracks well, and the waving motion along the curve is due to periods along the flight path where the higher velocity generates more lift and lowers the flight path angle. The curve flattens and the vehicle flies a long period of time at a shallower flight path angle. It takes longer time to descend to the next interval altitude and much of the velocity is removed by the end of the interval. As the vehicle slows, it descends more rapidly and the time

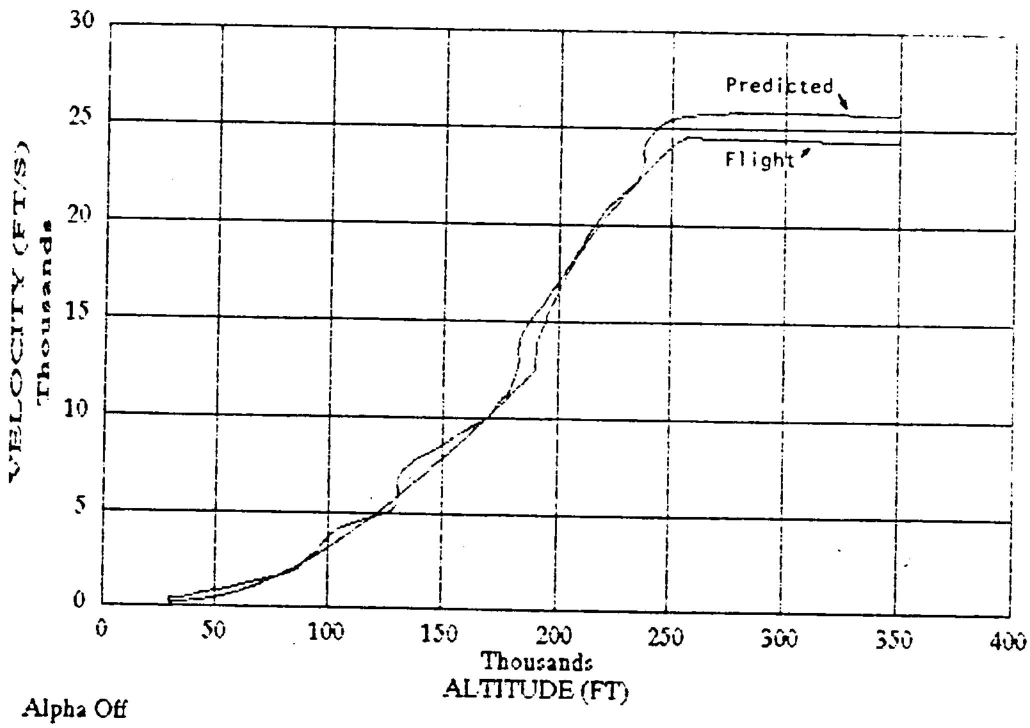

Figure 23. Predicted and Flight Velocities STS-4

until the next interval is reached is shortened. This results in an epoch in which relatively less of the velocity is lost. This motion Continues down to 31,000 ft where the vehicle is predicted to begin to ascend vertically.

Hankey (7) describes this motion as hypersonic phugoid. Large low frequency oscillations develop for shallow flight path angle lifting reentries. The behavior is expected, and its appearance in the prediction is welcome.

A clearer picture of the flight path angle situation is shown in Figure 24. Here the shuttle tracks along a very shallow flight path angle very close to constant altitude flight to about 170,000 ft. The shuttle then descends, and then begins to level off, peaking at 135,000 ft, then again falling off. At 45,000 ft the shuttle has lost most of its original velocity and the erratic behavior is predicted. If this is real, the shuttle's attitude control system would provide control inputs to damp this motion. At the very end a dramatic flight direction change is postulated and the shuttle heads vertically upward.

The final parameter investigated is the loading. Here a very smooth reentry ride is shown in Figure 25. The load begins in the vicinity of 1 g until 220,000 ft, where it rises and oscillates about 1.5 g to 130,000 ft. It again hovers about 1 g until 90,000 ft, where the crew are then predicted to obtain a near weightless environment. This result is consistent with the low g reentry claims though comparisons of load data were not found.

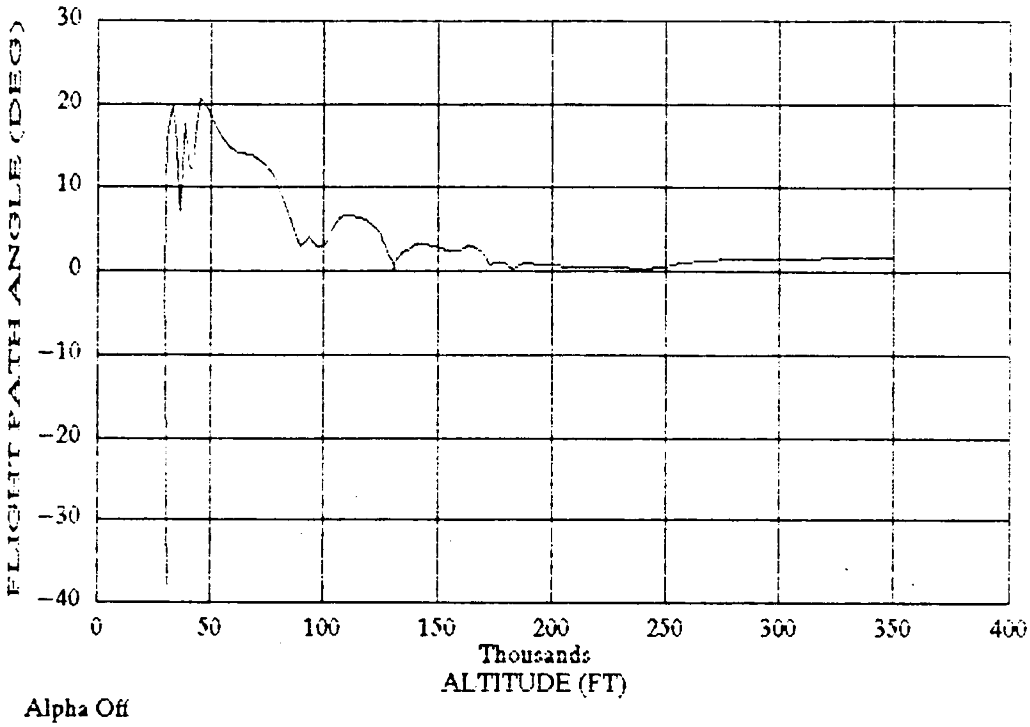

Figure 24. STS-4 Predicted Flight Path Angle

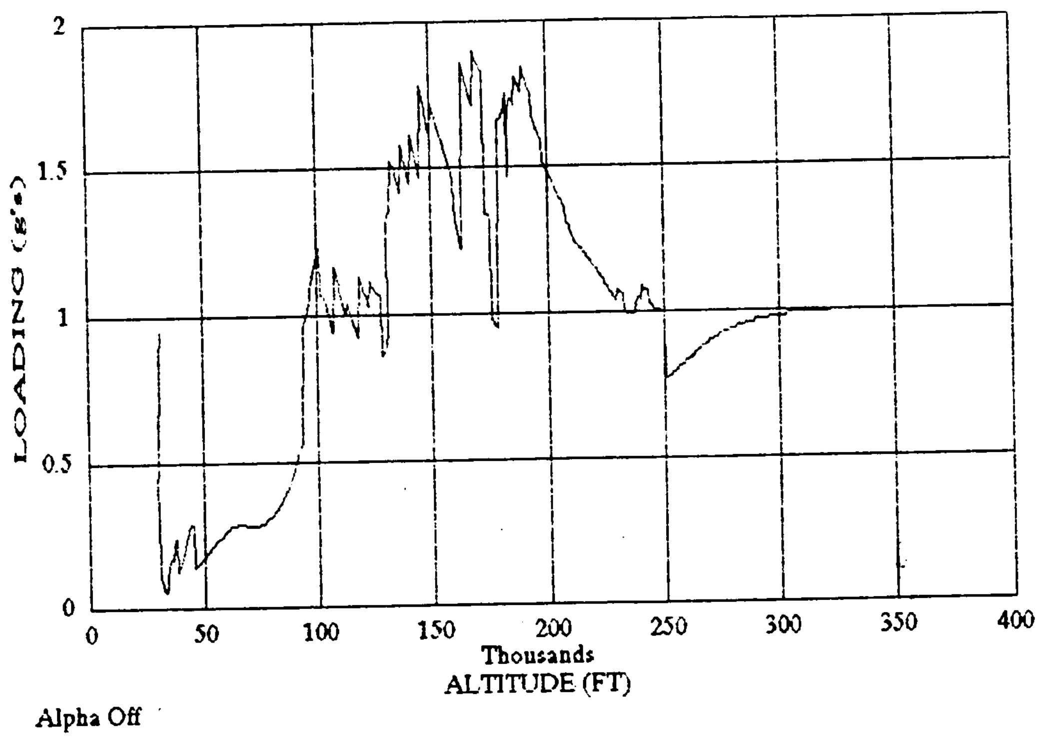

Figure 25. STS-4 Predicted Loading

The program contains provisions to fix the reentry velocity to any given value. This option was selected by going into the ORBT.DAT table, changing the velocity fix on/off flag from a 0 to a 1, and Changing the velocity from 0 to 24,431 ft/s. The program was then rerun.

Figure 26 shows a comparison of the new velocity prediction to the flight data curves. The prediction forecasts the shuttle would depart on a large skip trajectory at 200,000 ft, carrying it to an altitude of 310,000 ft, before again descending to the surface.

On either side of this skip there are two large regions where the shuttle is predicted to retain a constant velocity as it descends. Apparently, at the lower velocity, enough lift and drag cannot be generated to affect the flight path angle, until the greater atmospheric density of the lower altitude can increase the magnitude of the aerodynamic forces. At 200,000 ft the velocity is actually higher for the slower reentry. The lift force is in a more unstable relation with gravity and a more energetic skip occurs.

The data presented after the skip is of dubious value. Here the shuttle descends 200,000 ft at constant velocity, until the lift and drag terms can kick in and begin to rob the vehicle of more of its speed during a given interval. At 100,000 ft it tracks well with the flight data. This prediction may indeed be valid, but it will not be proven.

The nature of the relationship of the change in velocity with respect to altitude is further explored. The derivative of the

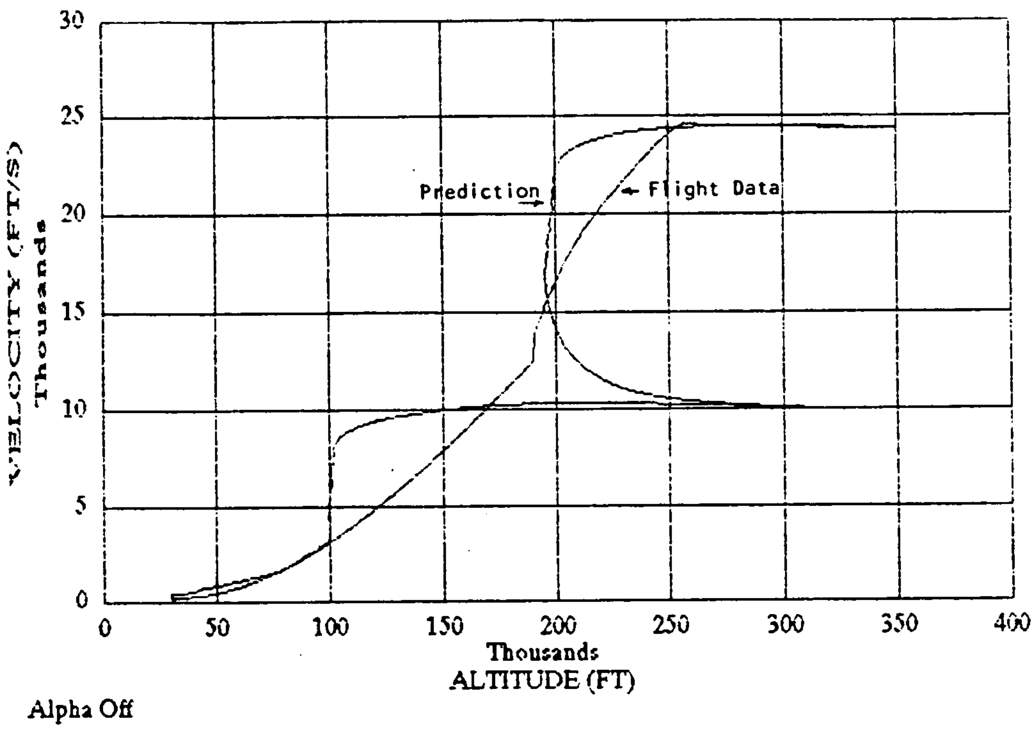

Figure 26. STS-4 Forced Velocity Prediction

velocity with respect to altitude was determined from the momentum equation. The sum of the forces equals the time rate of change of momentum:

$$\mathbf{F} = d\mathbf{P}/dt$$

But, the sum of the forces are the lift, drag, and gravity:

$$\mathbf{L} + \mathbf{D} + \mathbf{g} = m d\mathbf{V}/dt$$

since the mass is constant. Looking now only at the magnitude of these vectors:

$$(L^2 + D^2 + g^2)^{1/2} = m\, dV/dz\; dz/dt$$

From earlier calculations it will be remembered:

$$dz/dt = -V \sin\gamma \cos\alpha = -V \sin\gamma$$

where $\alpha = 0$.

$$dV/dz = \left[\left(\frac{C_L \rho V^2 S}{2MV \sin\gamma}\right)^2 + \left(\frac{C_D \rho V^2 S}{2mV \sin\gamma}\right)^2 + \left(\frac{g}{mV \sin\gamma}\right)^2\right]^{1/2}$$

$$= \left[\left(\frac{g\rho VK}{2\beta \sin\gamma}\right)^2 + \left(\frac{g\rho V}{2\beta \sin\gamma}\right)^2 + \left(\frac{g}{mV \sin\gamma}\right)^2\right]^{1/2}$$

$$= g\left[\left(\frac{\rho V}{2\beta \sin\gamma}\right)^2 (1+K^2) + \frac{1}{mV \sin\gamma}\right]^{1/2}$$

$$dV/dz = \frac{g_o}{MV(1+z/R_E)^2 \sin\gamma}\left[\left(\frac{mV^2\rho}{2\beta}\right)^2 (1+K^2) + 1\right]^{1/2}$$

This is the equation graphed in Figure 27. It demonstrates the very gentle velocity gradients, except at the two points near 200,000 ft and 100,000 ft where the huge gradients exist in Figure 26. Figure 28 shows how the function one over the sin γ demonstrates the same behavior at those two altitudes as the dV/dz curve does. In Figure 29 the gradient curve without the gamma function is plotted. The excursion at 200,000 ft is absent, indicating the change in velocity with respect to altitude is largely a function of the flight path angle, as anticipated.

This comparison between the two reentry predictions demonstrate the complex interaction between, and great sensitivity of, the various reentry parameters. Caution is advised in dismissing the second result too. Perhaps some small control input at 250,000 ft would align this predicted profile much closer with the flight data. The interplay is very dynamic, and small changes in reentry conditions may have a very large impact upon the predicted results, as has just been demonstrated.

The flight path angle variation is presented in Figure 30. Here the prediction tracks along a shallow glide slope and into the skip loop. Out of the skip the angle steepens until at 100,000 ft, where the velocity falls off precipitously. The curve then falls, oscillates, and finally goes divergent at 30,000 ft.

The loading curve, Figure 31, demonstrates the expected type of behavior. Staying close to 1 g, it proceeds through the loop caused by the skip, then increases steadily to to 6.5 g's at 100,000 ft. The

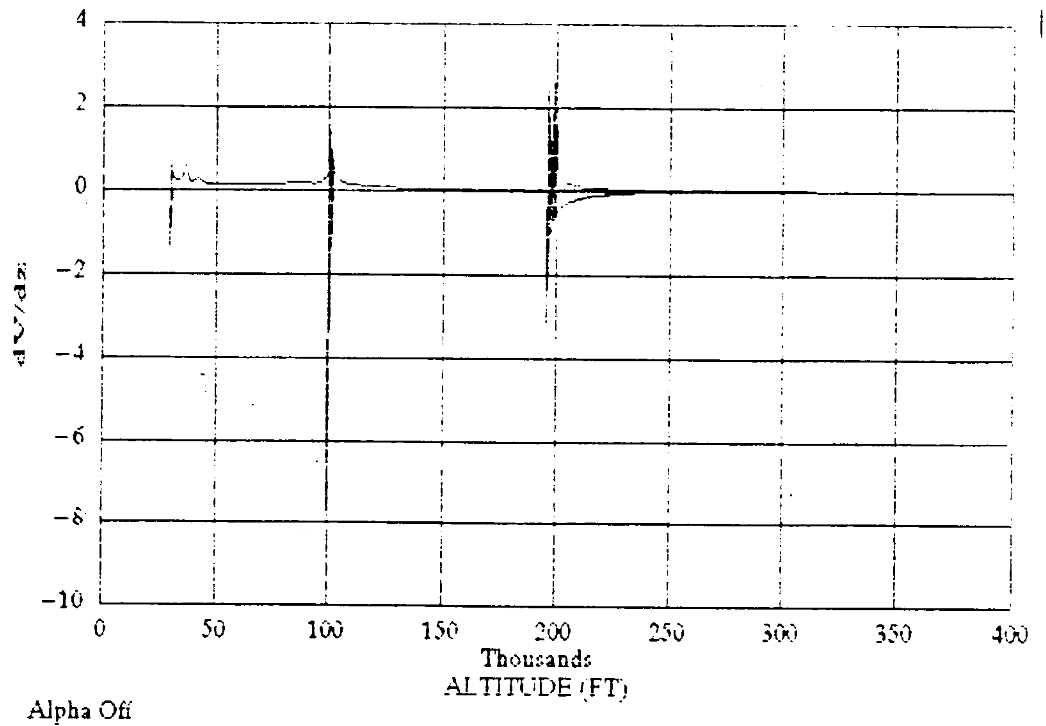

Figure 27. Velocity Derivative

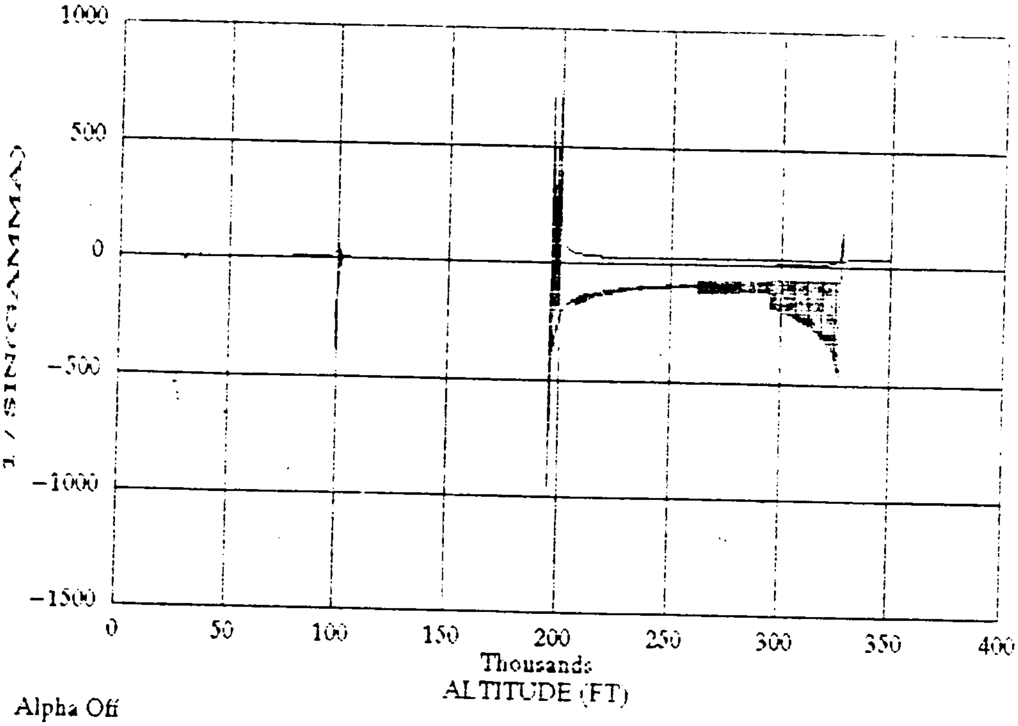

Figure 28. Flight Path Angle Function versus Altitude

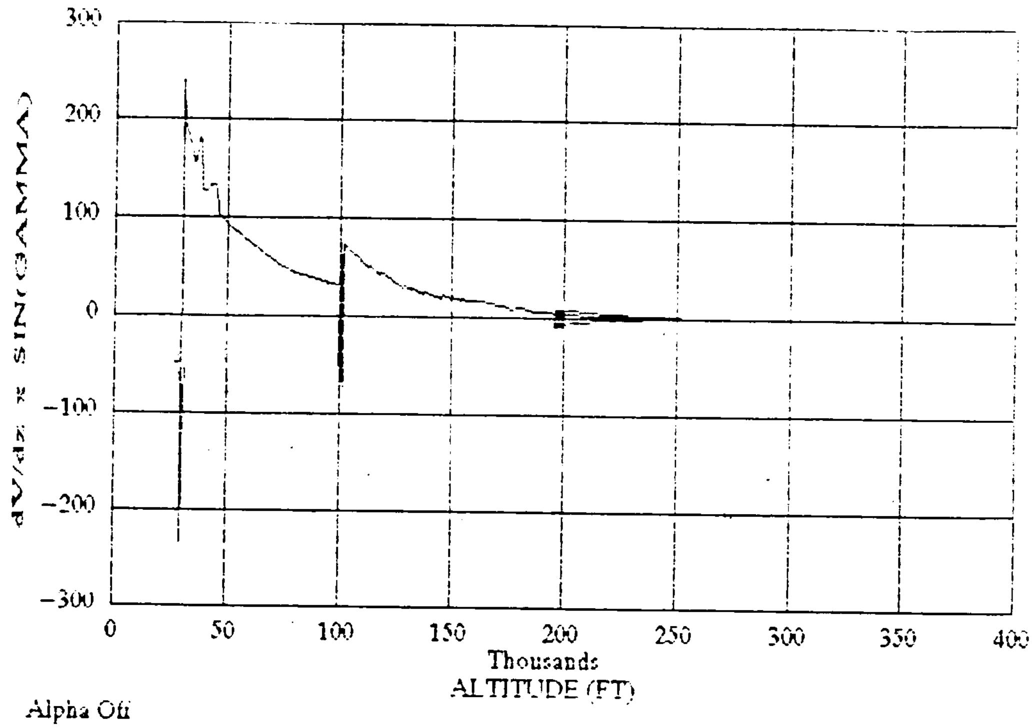

Figure 29. Derivative Minus Flight Path Angle Function

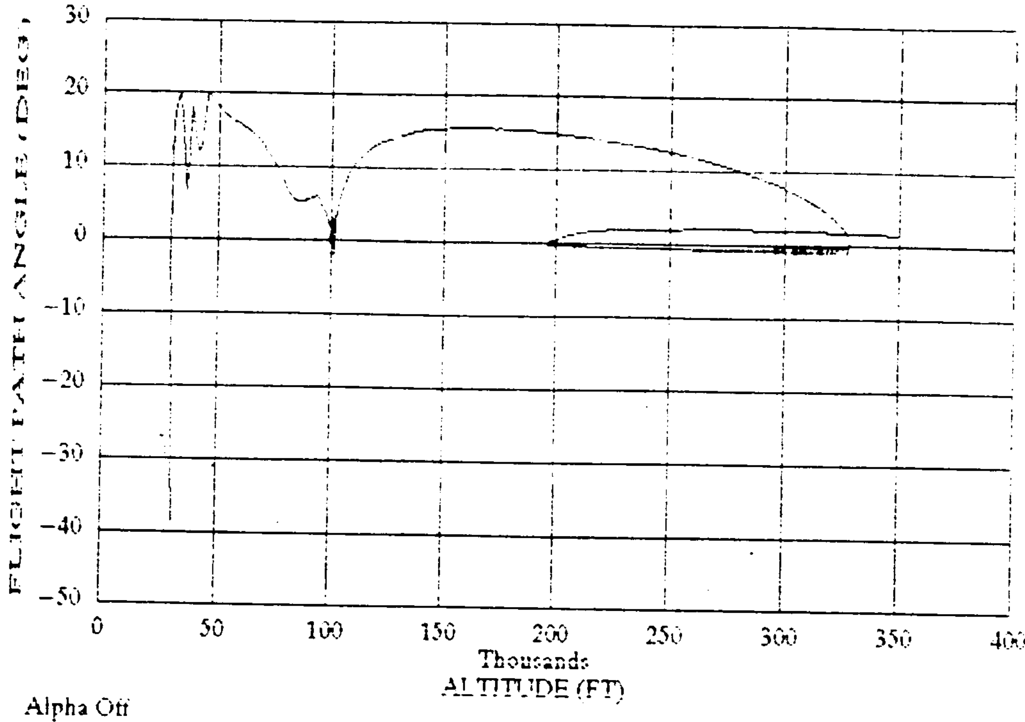

Figure 30. STS-4 Forced Velocity Flight Path Angle

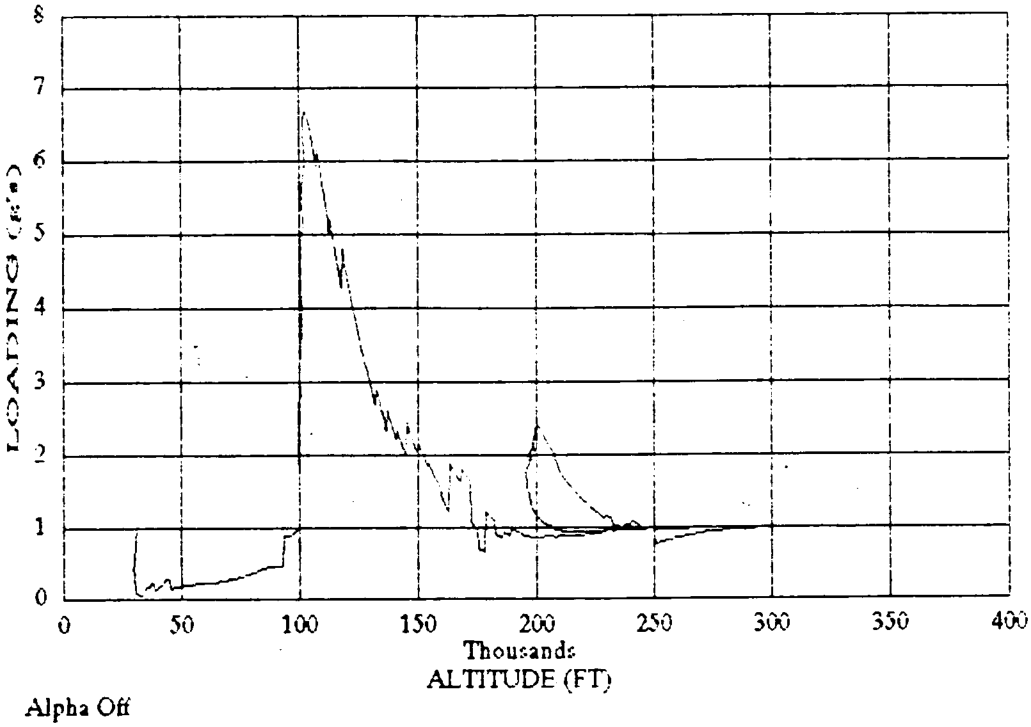

Figure 31. STS-4 Forced Velocity Loading

loading then falls off rapidly and remains near 0.5 g for the remainder of the flight.

It is possible the measured flight velocity is too low. If it measured higher than actual, the prediction may show even greater differences. The contention is not to explain the 5.6% difference between predicted entry velocity and actual entry velocity as instrumentation error, but rather to hypothesize if any instrument error was present, if may have been in that direction.

Another, greater, possibility is that the density function understates the actual density at higher altitudes. By modifying the density function, the velocity can be made to track much better compared to the flight data, as shown in Figure 32. Figure 33 shows the density factor curve. This is the amount the density is multiplied by while executing the program. Below 230,000 ft there is no change to the density, but between 230,000 and 250,000 ft the density factor changes almost linearly from one to three. Above this altitude the atmosphere apparently becomes so rarified there is negligible aerodynamic force acting on the vehicle.

No hard evidence was found to support the conclusion the 1962 US Standard Atmosphere Model is wrong at these altitudes. However, Dubin (6) has indicated large variations either diurnal or seasonal have been demonstrated to exist, which would validate a significant fraction of this difference. These fractions are on the order of 40 percent.

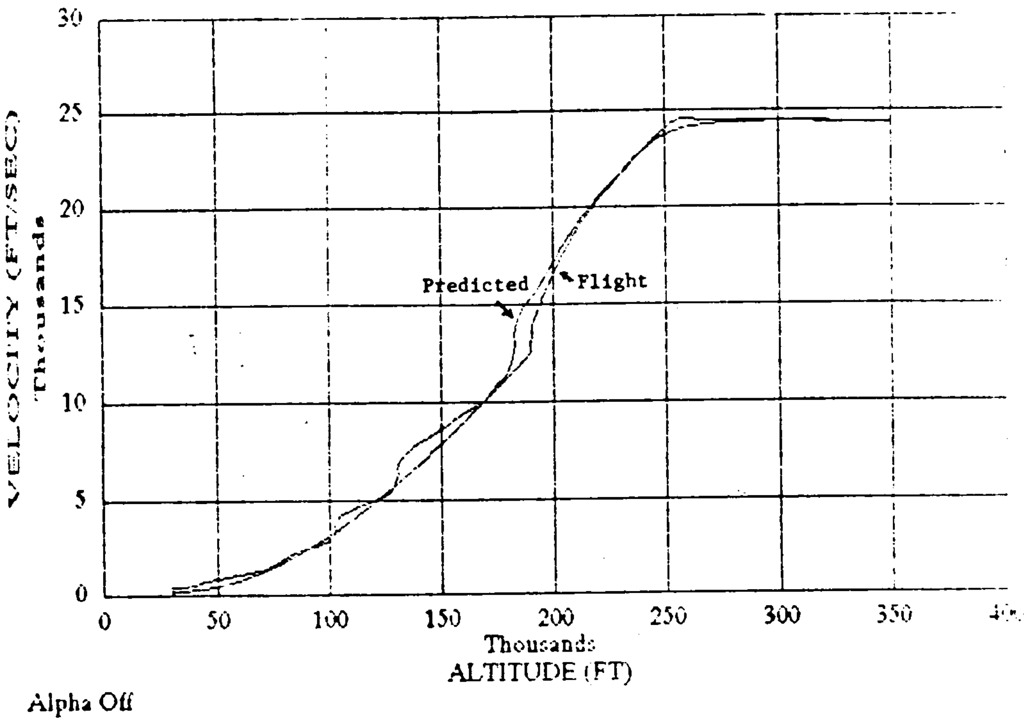

Figure 32. STS-4 Forced Velocity with Density Augmentation

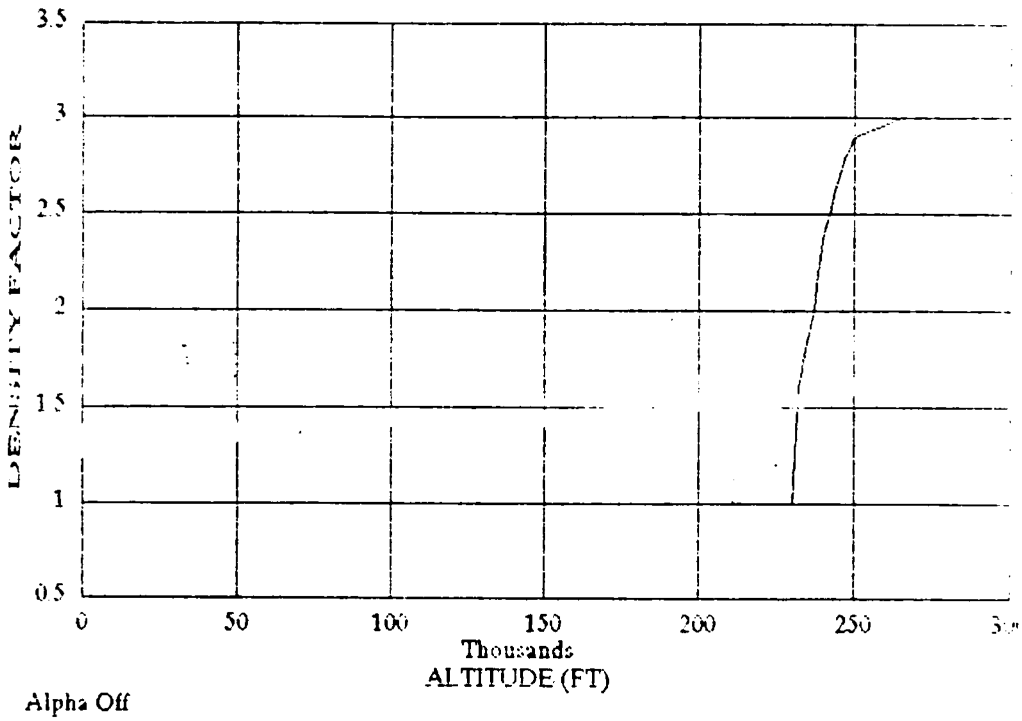

Figure 33. Density Factor versus Altitude

Forty percent is a long way from 300 percent, but it does open the possibility that the Tables may be in error. Some data on the very low level shuttle missions have indicted the density is higher than predicted by the 1962 US Standard Atmosphere. It remains an area requiring further investigation before density errors can be discounted.

CHAPTER 5

SMALL SATELLITE REENTRY PREDICTION

How would a typical small satellite fare in the predictive program? Among the developing space systems are the Pegasus and Taurus launch systems. These represent the new breed of small, inexpensive, space systems. The Pegasus system, built by Orbital Sciences Corporation, is designed to be carried aloft, under the wing of a large transport aircraft, and launched. Currently using a B-52, the Pegasus system is undergoing flight trials now.

Once in orbit, a portion of the payload is designed to separate, and return to Earth. This return vehicle, called Freeflyer, will house the recoverable payload, and must survive the reentry and impact loads.

To run the program, INPUT.FOR requires the space vehicle and orbital specifications. A fictitious vehicle was created and input into the program. Figure 34 shows the ORBT.DAT and LTD.DAT files generated. The reentry is proposed to begin at 350,000 ft like the shuttle. The orbit is 150 x 180 nautical miles, and the reentry angle is three degrees. The vehicle was a 50 lb, 16 inch sphere, which translates into a mass of 1.553 slugs, and a reference area of 1.396 ft^2.

The LTD.DAT table was constructed very simply: The drag coefficient was assumed to be 0.27 over the entire flight regime, and the lift coefficient was assumed to be 0.1. No bank angle was employed. The program was run and the results tabulated in file LOAD. DAT.

350000.0000000	
150.0000000	180.0000000
3.0000000	
.0000000	.0000000
1.5530000	
1.3960000	
1000.0000000	
10000.0000000	
1.0000000	

400000.	.10	.27	.37	.0
0.	.00	.00	.00	.0

Figure 34. Small Satellite Input Data Files

Figure 35 shows the velocity profile for the reentry. The velocity holds constant at 25,000 ft/s until an altitude of 180,000 ft is reached. As has been seen before, the velocity then falls off very rapidly until it reaches 13,000 ft/s, then continues to decline more slowly with altitude. The curve softens out at 100,000 ft.

The flight path angle curve, Figure 36, is very steady until a slight skip at 165,000 ft, then falls off easily to nearly 70 degrees at 10,000 ft.

The loading curve shown in Figure 37, shows a double peak situation. The first peak, at 170,000 ft is due to the high velocity generating large aerodynamic forces on the body. The velocity chart in Figure 35 shows the velocity then falls off precipitously, and so would the forces. The next, smoother hump at 130,000 ft is due to the increasing density driving up the aerodynamic forces. As the vehicle continues to slow, this force also diminishes.

An identical run was made, except the flight path angle has been increased to 10 degrees. In Figure 38 the reentry velocity begins at a much lower 22,000 ft/s. This is due to the fact the perigee must be much closer to the surface of the Earth to provide a 10 degree flight path angle at 350,000 ft. The delta v for the 3 degree case was 668 ft/s, while the delta v here was 4,545 ft/s. Much more of the energy was bled by the deorbit maneuver.

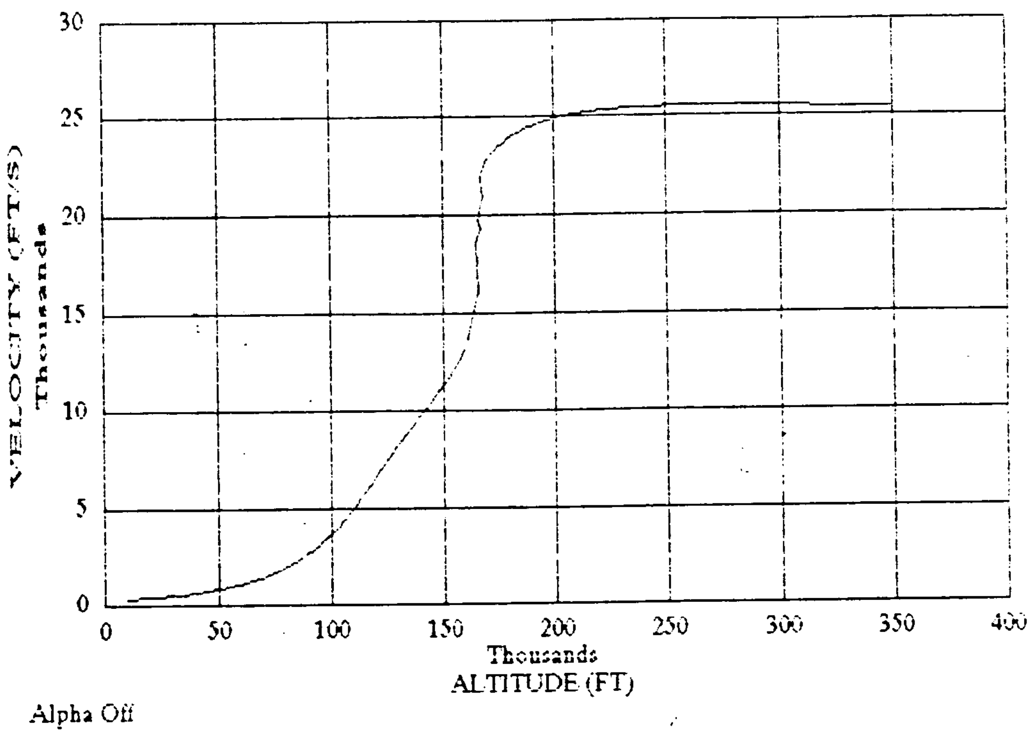

Figure 35. Freeflyer Predicted Velocity 3 Degrees

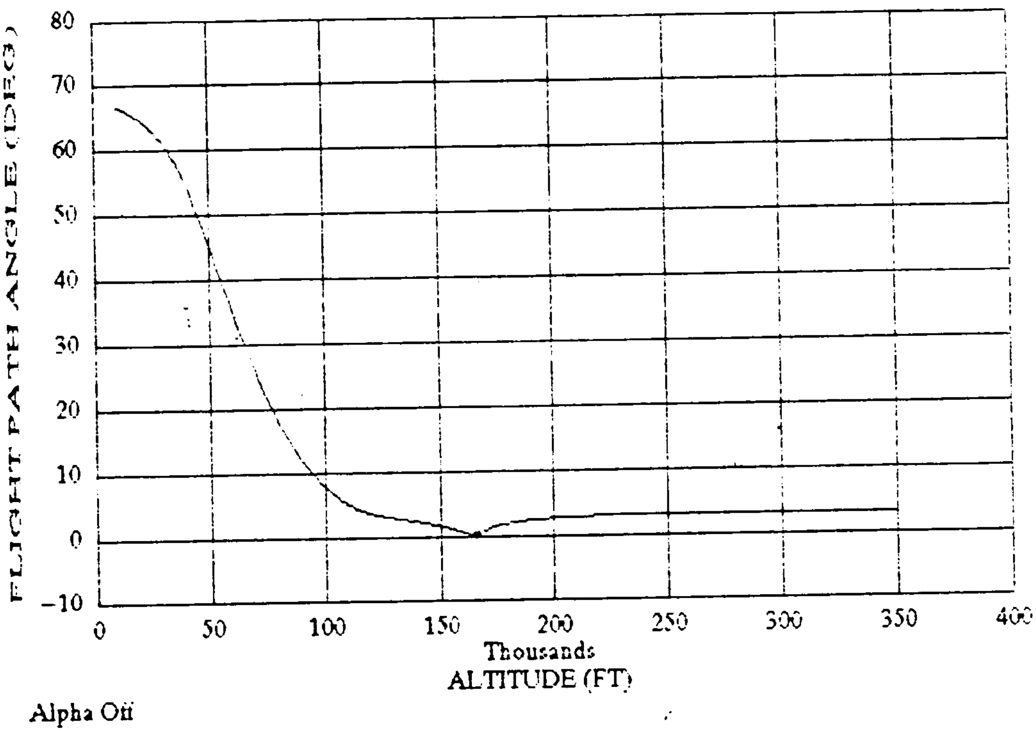

Figure 36. Freeflyer Predicted FPA 3 Degrees

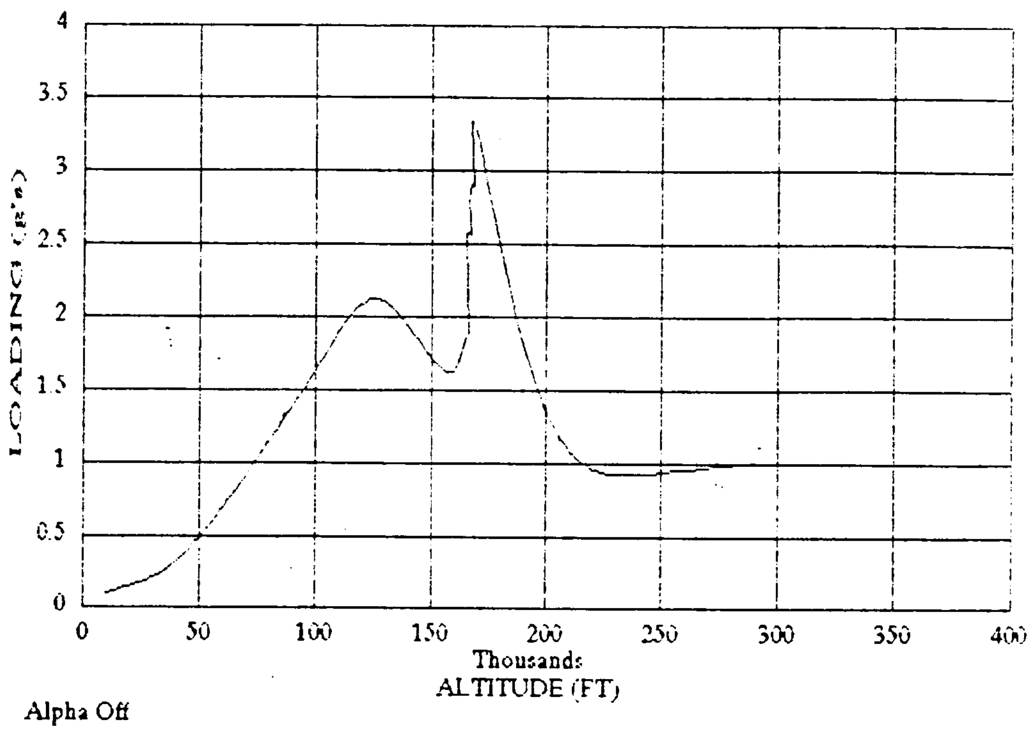

Figure 37. Freeflyer Predicted Loading 3 Degrees

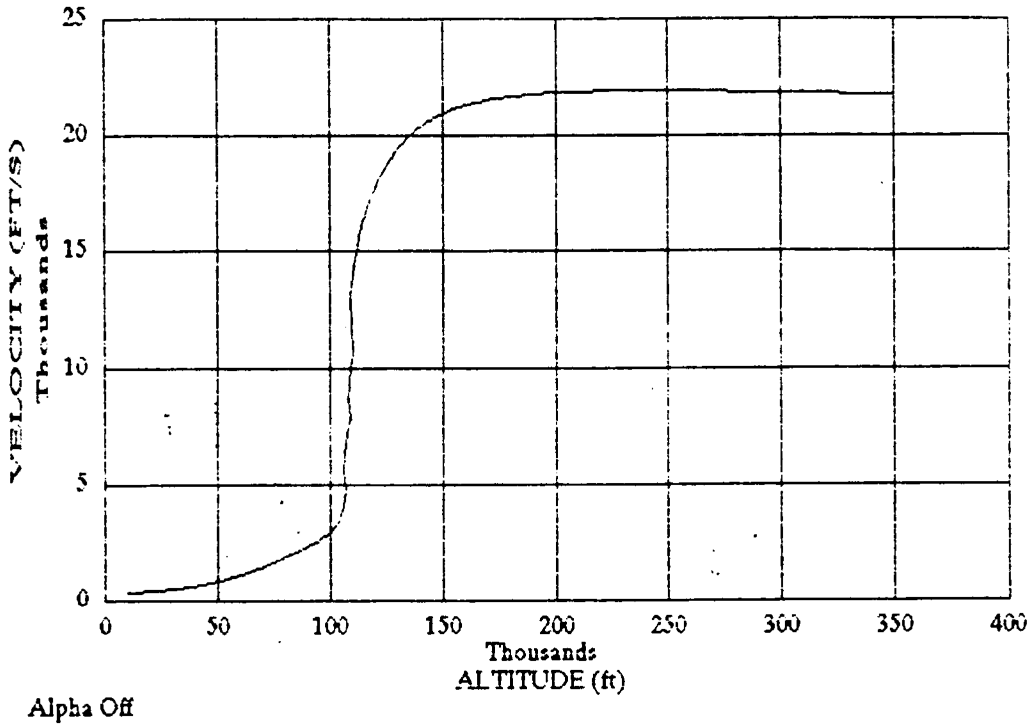

Figure 38. Freeflyer Predicted Velocity 10 Degrees

With a steeper reentry more of the velocity was maintained until the vehicle descended to 120,000 ft, where the vehicle braked continuously until the velocity fell below 4,000 ft/s, and flaired off. Lower velocity means deeper atmospheric penetration until the drag force becomes sufficient to retard the motion.

The flight path angle curve in Figure 39 shows the behavior of the rapid decline in velocity accompanied by a rise in the flight path angle. There is a slight skip at 110,000 ft, then steady increase in angle, reminiscent of a ballistic reentry. Finally, Figure 40 shows the two load peaks superimposed upon one another. Here the velocity and density combine to create a larger load peak at 120,000 ft. Notice the difference in magnitudes: the shallow angle reentry experiences a maximum loading of 3.3 g's, while the steeper reentry obtains a 17.4 g loading.

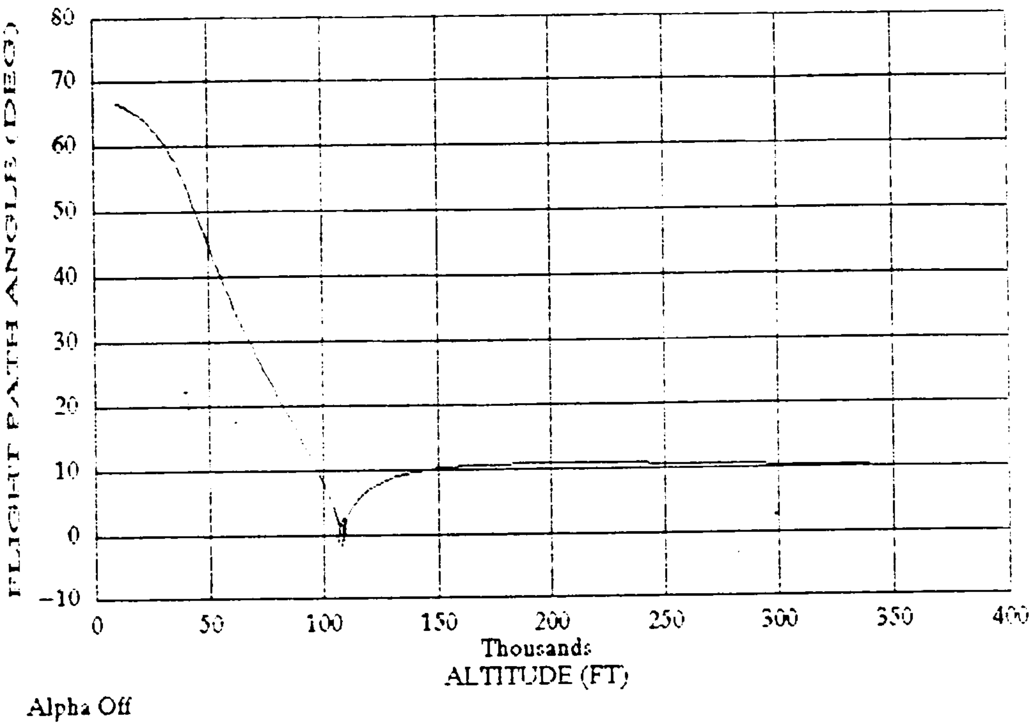

Figure 39. Freeflyer Predicted FPA 10 Degrees

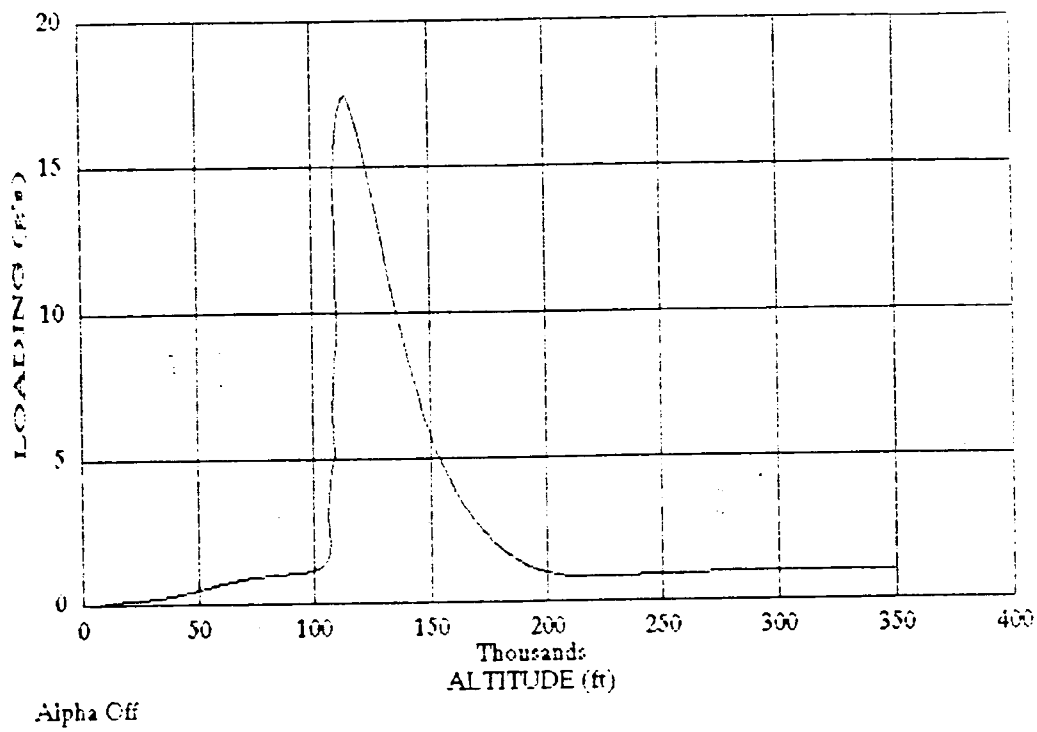

Figure 40. Freeflyer Predicted Loading 10 Degrees

CHAPTER 6

CONCLUSIONS

The purpose of the thesis was to develop and demonstrate a reentry parameter prediction routine for use on a personal computer. The program was written and validated against a very complicated reentry of the U. S. Space Shuttle. The program runs quickly on the host computer (Unisys Personal Workstation Series 800/16), and as a result many different reentry scenarios may be run in a very short time. The software does have some limitations. It is not designed to handle wild skip trajectories. The very moderate skip oscillation is believed to be adequately modeled, but confidence in the accuracy of the prediction falls off as swiftly as the rate of skip rises. Also a blind spot does exist in the program which shows a singularity should the vehicle attempt to fly a true constant altitude trajectory.

It has been demonstrated at low flight path angles, the reentry physics tends to diverge rapidly and small changes to the input parameters may have large effects on the trajectory. Care should be exercised in dismissing solutions since small input modifications may settle the responses down. It is especially recommended the program operator try a smaller altitude interval, in that convergence may be the problem. As an extra the density of the atmosphere was derived mathematically and those results were found to be in excellent agreement with the tabulated data in the 1962 U. S. Standard Atmosphere.

The validity of the density at altitudes near 250,000 ft are questionable, and bear further investigation.

LIST OF REFERENCES

LIST OF REFERENCES

1. Ely, Lawrence D., Return From Space, Springfield, IL: Charles Thomas, 1966.

2. Woods, W. C., Arrington, J. P., Hamilton, H. H., "A Review of Preflight Estimates of Real-Gas Effects on Space Shuttle Aerodynamic Characteristics", NASA Conference Publication 2283 Part I, Hampton, VA: NASA, 1983.

3. Bray, K. N. C., "Real Gas Effects On Lifting Reentry Aerothermodynamics", AGARD Lecture Series No. 42, Vol. 1, London: AGARD, 1972.

4. Regan, Frank J., Reentry Vehicle Dynamics, New York, NY: AIAA, 1984.

5. Wiesel, William E., Spaceflight Dynamics, New York, NY: McGraw-Hill Books, 1989.

6. Dubin, Maurice, Editor, U. S. Standard Atmosphere, 1962, National Aeronautics and Space Administration, Washington, DC: U. S. Government Printing Office, 1962.

7. Hankey, Wilbur L., Reentry Aerodynamics, Washington, DC: AIAA, 1988.

8. Craig, Richard A., The Upper Atmosphere, New York, NY: Academic Press, 1965.

9. Dubin, Maurice, Editor, U. S. Standard Atmosphere Supplements, 1966, Environmental Science Services Administration, Washington, DC: U. S. Government Printing Office, 1966.

10. Groves, G. V., McDermott, D. P., "Variations in the Earth's Atmospheric Structure, 30 to 250 Km", Dynamics of Manned Lifting Planetary Entry, New York, NY: John Wiley & Sons, 1963.

11. Ehricke, Krafft A., Space Flight, Princeton, NJ: D. van Nostrand Company, 1962.

12. Duncan, Robert Clifton, Dynamics of Atmospheric Entry, New York, NY: McGraw-Hill Books, 1962.

13. Kork, Jyri, "Satellite Reentry", Design Guide to Orbital Flight, New York, NY: McGraw-Hill Books, 1962.

14. Tucker, Maurice, "Spacecraft Entry and Landing in Planetary Atmospheres", Advances in Space and Science Technology, Vol. 4, New York, NY: Academic Press, 1962.

15 Romere, Paul O., Whitnah, A. Miles, "Space Shuttle Entry Longitudinal Aerodynamic Comparisons of Flights 1-4 with Preflight Predictions", NASA Conference Publication 2283 Part I, Hampton, VA: NASA, 1983.

16. Bate, Roger R., Mueller, Donald D., White, Jerry E., Fundamentals of Astrodynamics, New York, NY: Dover, Publications, 1971.

17. Loh, W. H. T., Reentry and Planetary Entry Physics and Technology Dynamics, Physics, Radiation, Heat Transfer, and Ablation, New York, NY: Springer-Verlag, 1968

18. Murphy, J., Ridout, D., McShane, Brigid, Numerical Analysis, Algorithms and Computation, New York, NY: Halsted Press, 1988.

19. Compton, Harold R., Schiess, James R., Suit, William T., "Stability and Control Over the Supersonic and Hypersonic Speed Range", NASA Conference Publication 2283, Part I, Hampton, VA: NASA, 1983.

20. Thompson, Tina D., Editor, Space Log 1957-1987, Vol. 23, Redondo Beach, CA: TRW, 1988.

21. Joels, Kerry Mark, Kennedy, Gregory P., Larkin, David, The Space Shuttle Operator's Manual, New York, NY: Ballantine Books, 1982.

22. Bennet, Dale E., "Space Shuttle Entry Flight Overview", Advances in the Astronautical Sciences, Vol. 51, San Diego, CA: Univelt, Inc., 1983.

23. Gradshteyn, I. S., Ryzhik, I. M., Tables of Integrals Series and Products, New York, NY: Academic Press, 1965.

APPENDICES

APPENDIX A

DENSITY DERIVATION

Beginning with the hydrostatic equation, and the ideal gas law:

$$\frac{dP}{dz} = -\rho g \quad and \qquad P = \rho RT$$

Substituting to obtain:

$$\frac{d(\rho RT)}{dz} = \frac{RTd\rho}{dz} + \frac{\rho RdR}{dz} + \frac{\rho RdT}{dz} = -\rho g$$

Assume dR/dz = 0, R = constant

$$\frac{RTd\rho}{dz} + \frac{\rho RdT}{dz} = -\rho g$$

$$\frac{1}{\rho}\frac{d\rho}{dz} + \frac{1}{T}\frac{dT}{dz} = \frac{-g}{RT}$$

T, g are functions of z. T is a linear function, and g is a quadratic function:

$$T(z) = p + qz, g(z) = g_o(1 + z/R_E) - 2$$

Find some function u(z), such that du/dz = g(z), or

$$u(z) = g(z)dz = -g_o R_E (1 + z/R_E)^{-1}$$

It can then be written:

$$\frac{1}{\rho}\frac{d\rho}{dz} + \frac{1}{T}\frac{dT}{dz} = \frac{-1}{RT}\frac{du}{dz}$$

$$\frac{d\rho}{\rho} + \frac{dT}{T} = \frac{-du}{RT}$$

$$\int \frac{d\rho}{\rho} + \int \frac{dT}{T} = \frac{-1}{R} \int \frac{du}{T}$$

$$\ell n\rho + \ell nT = \frac{-1}{R} \int \frac{du}{T} + C$$

$$= -\,1/R \int (p+qz)^{-1} g_o (1+z/R_E)^{-2}\, dz$$

$$= -\, g_o/R \int (p+qz)^{-1} (1+2z/R_E + (z/R_E)^2)^{-1}\, dz$$

From a table of integrals in Gradshteyn (23), a solution was found to the equation form:

$$\int \frac{dx}{zR} = \frac{\beta}{2A} \ell n \frac{z^2}{R} - \frac{B}{2A} \int \frac{dx}{R}$$

Where,

$$R = a + bx + cx^2, z = \alpha + \beta x$$

and,

$$A = a\beta^2 - ab\beta + c\alpha^2, \quad B = b\beta - 2c\alpha$$

Therefore,

$$\int \frac{dz}{(p+qz)(1+2z/R_E + (p/R_E)^2}$$

$$= \frac{q}{2(q^2 - 2qp/R_E + (p/R_E)^2)} \ell n\, ((p+qz)/(1+z/R_E))^2$$

$$- \frac{((g/R_E) - 2p/(R_E)^2)\, R_E (1+z/R_E)^{-1}}{2(q^2 - 2qp/R_E + (p/R_E)^2)} + C.$$

Evaluated at two points:

$$\ell n\left(\frac{\rho_2}{\rho_1}\right) + \ell n\left(\frac{T_2}{T_1}\right) = \frac{-g_o q}{2R(q^2 - 2qp/R_E + (p/R_E)^2)}\, x$$

$$\left(\ell n\left[\frac{(p+qz_2)(1+z_1/R_E)}{(p+qz_1)(1+z_2/R_E)}\right]^2 + \frac{(1-2p/qR_E)(z_1-z_2)}{R_E(1+z_2/R_E)(1+z_1/R_E)}\right)$$

for the final solution:

$$\rho_2 = \rho_1 \frac{p+qz_1}{p+qz_2}\, exp\left\{\frac{-g_o}{2R(q^2 - 2qp/R_E + (p/R_E)^2)}\, x\right.$$

$$\left.\left(q\,\ell n\left[\frac{(p+qz_2)(1+z_1/R_E)}{(p+qz_1)(1+z_2/R_E)}\right]^2 + \frac{(q-2p/R_E)(z_1-z_2)}{R_E(1+z_2/R_E)(1+z_1/R_E)}\right)\right\}.$$

APPENDIX B

NUMERICAL INTEGRATIONS

The numerical solution used is built around the Taylor Series solution, which is a derivative series solution designed, according to Murphy (18), for the initial value problem. The key factor to watch for when applying this technique is that the series does converge to a solution. The technique begins with the definition of the Taylor Series Expansion.

$$y(x_o + \Delta x) = x_o + \frac{\Delta z}{1!}\dot{x}_o + \frac{\Delta z^2}{2!}\ddot{x}_o + \ldots + \frac{\Delta z^n}{n!}x_o^{(n)}.$$

To find the solution at the next interval the initial value at the interval, plus the initial values of the derivatives are required. The velocity equation is in the form:

$$\frac{d\lambda}{d\rho} = \frac{2gH}{R_E g_o \rho} - \frac{g\lambda H}{\beta \sin\gamma \cos\alpha}$$

By combining the constants to remove the clutter the equation is restated as:

$$\frac{d\lambda}{d\rho} = D\rho^{-1} - C\lambda$$

The following derivatives are easily determined:

$$\frac{d^2\lambda}{d\rho^2} = -D\rho^{-2} - \frac{Cd\lambda}{d\rho}$$

$$\frac{d^3\lambda}{d\rho^3} = -2D\rho^{-3} - \frac{Cd^2\lambda}{d\rho^2}$$

$$\frac{d^4\lambda}{d\rho^4} = -6D\rho^{-4} - \frac{Cd^3\lambda}{d\rho^3}$$

$$\frac{d^5\lambda}{d\rho^5} = -24D\rho^{-5} - \frac{Cd^4\lambda}{d\rho^4}$$

$$\frac{d^6\lambda}{d\rho^6} = -120D\rho^{-6} - \frac{Cd^5\lambda}{d\rho^5}$$

$$\frac{d^7\lambda}{d\rho^7} = -720D\rho^{-7} - \frac{Cd^6\lambda}{d\rho^6}.$$

It is easy to solve for for each derivative, then plug into the next equation. The x_0 terms have now been solved for, but what of the Δx terms? These are merely the changes in density. The computer generates this number in subroutine DELT as the variable DRO. The value of at the next interval is:

$$\lambda_f = \lambda_i + \frac{\Delta\rho d\lambda}{1!\,d\rho} + \frac{\Delta\rho^2 d^2\lambda}{2!\,d\rho^2} + \frac{\Delta\rho^3 d^3\lambda}{3!\,d\rho^3} + \frac{\Delta\rho^4 d^4\lambda}{4!\,d\rho^4} + \frac{\Delta\rho^5 d^5\lambda}{5!\,d\rho^5} + \frac{\Delta\rho^6 d^6\lambda}{6!\,d\rho^6} + \frac{\Delta\rho^7 d^7\lambda}{7!\,d\rho^7}$$

The solution for w works in the same way. Start by collecting the constants:

$$\frac{dw}{d\rho} = \frac{-wH}{(R_E+z)}\left[\frac{R_E}{\lambda(R_E+z)\cos^2\alpha} - 1\right] + \frac{gHK\cos\alpha}{2\beta\cos^2\alpha}$$

$$\frac{dw}{d\rho} = D - C\rho^{-1}w$$

The derivatives follow:

$$\frac{d^2w}{d\rho^2} = C\rho^{-2}w - C\rho^{-1}\frac{dw}{d\rho}$$

$$\frac{d^3w}{d\rho^3} = -2C\rho^{-3}w + 2C\rho^{-2}\frac{dw}{d\rho} - C\rho^{-1}\frac{d^2w}{d\rho^2}$$

$$\frac{d^4w}{d\rho^4} = 6C\rho^{-4}w - 6C\rho^{-3}\frac{dw}{d\rho} + 3C\rho^{-2}\frac{d^3w}{d\rho^3}$$

$$\frac{d^5w}{d\rho^5} = -24C\rho^{-5}w + 24C\rho^{-4}\frac{dw}{d\rho} - 12C\rho^{-3}\frac{d^2w}{d\rho^2} + 4C\rho^{-2}\frac{d^3w}{d\rho^3} - C\rho^{-1}\frac{d^4w}{d\rho^4}$$

$$\frac{d^6w}{d\rho^6} = 120C\rho^{-6}w - 120C\rho^{-5}\frac{dw}{d\rho} + 60C\rho^{-4}\frac{d^2w}{d\rho^3} - 20C\rho^{-3}\frac{d^3w}{d\rho^3} + 5C\rho^{-2}\frac{d^4w}{d\rho^4} - C\rho^{-1}\frac{d^5w}{d\rho^5}$$

$$\frac{d^7w}{d\rho^7} = -720C\rho^{-7}w + 720C\rho^{-6}\frac{dw}{d\rho} - 360C\rho^{-5}\frac{d^2w}{d\rho^2} + 120C\rho^{-4}\frac{d^3w}{d\rho^3} - 30C\rho^{-3}\frac{d^4w}{d\rho^4} + 6C\rho^{-2}\frac{d^5w}{d\rho^5} - C\rho^{-1}\frac{d^6w}{d\rho^6}.$$

The same procedure is carried out to solve for the w variable at the end of the interval:

$$w_f = w_i + \frac{\Delta\rho dw}{1!\,d\rho} + \frac{\Delta\rho^2 d^2w}{2!\,d\rho^2} + \frac{\Delta\rho^3 d^3w}{3!\,d\rho^3} + \frac{\Delta\rho^4 d^4w}{4!\,d\rho^4} + \frac{\Delta\rho^5 d^5w}{5!\,d\rho^5} + \frac{\Delta\rho^6 d^6w}{6!\,d\rho^6} + \frac{\Delta\rho^7 d^7w}{7!\,d\rho^7}.$$

APPENDIX C

THE FORTRAN PROGRAMS

```
      PROGRAM INPUT
      REAL A,B,RA,CD,CL,K,S,FPAD,Z1,
      +STOP,INV,PS,M,Z,NK,FV,FA
C
C
      OPEN(6,FILE='ORBT.DAT',STATUS='NEW')
      REWIND 6
C
     NK=0
     WRITE(*,*) 'THIS PROGRAM WILL COMPUTE THE G LOADS ON
    +A SATELLITE RETURNING FROM LOW EARTH ORBIT.
    +ENTER THE FOLLOWING:'
     WRITE(*,*) 'INPUT INITIAL REENTRY ALT ESTIMATE'
     READ (*,*) Z1
     WRITE(6,*) Z1
     WRITE(*,*) 'INPUT APOGEE AND PERIGEE IN NAUTICAL
    +MILES'
     READ (*,*) A,B
     WRITE(6,*) A,B
     WRITE(*,*) 'WHAT IS THE DESIRED REENTRY ANGLE IN
    +DEGREES'
     READ (*,*) FPAD
     WRITE(6,*) FPAD
     WRITE(*,*) 'DO YOU WISH TO SPECIFY REENTRY VELOCITY?
    +1=Y,0=N'
     READ (*,*) FV
     IF (FV.EQ.1) THEN
        WRITE(*,*) 'WHAT IS THE DESIRED REENTRY VELOCITY,
    +   FT/S?'
        READ (*,*) VE
     ELSE
        VE=0.0
     ENDIF
     WRITE(6,*) FV,VE
     WRITE(*,*) 'INPUT REENTRY VEHICLE FLIGHT CHARACTERIS
    +TICS'
     WRITE(*,*) 'WHAT IS THE MASS(SLUGS)?'
     READ (*,*) M
     WRITE(6,*) M
     WRITE(*,*) 'WHAT IS REFERENCE AREA,FT2'
     READ (*,*) S
     WRITE(6,*) S
     WRITE(*,*) 'WHAT IS THE DESIRED ALTITUDE INTERVAL?'
     READ (*,*) INV
```

```
      WRITE(6,*) INV
      WRITE(*,*) 'INPUT THE LIFT AND DRAG TABLE'
      OPEN(2,FILE='LTD.DAT',STATUS='NEW')
      REWIND 2
      WRITE(*,*) 'WILL THE REENTRY VEHICLE BANK? (1=Y,0=N)'
      READ (*,*) NK
      WRITE(*,*) 'INPUT FLIGHT PROFILE.'
      A=0.0
500   WRITE(*,*) 'INPUT ALTITUDE (FT)'
      READ (*,*) Z
10    FORMAT(2X,F10.0,2X,F4.2,2X,F4.2,2X,F4.2,
     +2X,F5.1,2X,F5.2)
      IF (Z.GT.0) THEN
         IF (NK.EQ.1) THEN
            WRITE(*,*) 'INPUT CL, CD, AND BANK ANGLE'
            READ (*,*) CL,CD,PS
         ELSE
            PS=0
            WRITE(*,*) 'INPUT CL AND CD'
            READ (*,*) CL,CD
         ENDIF
         K=CL/CD
         WRITE(2,10) Z,CL,CD,K,PS
         GOTO 500
      ELSE
         WRITE(2,10) Z,A,A,A,A
      ENDIF
      WRITE(*,*) 'INPUT LOWEST ALTITUDE'
      READ (*,*) STOP
      WRITE(6,*) STOP
      WRITE(*,*) 'ASSUME ALPHA ZERO? 1=Y,0=N'
      READ (*,*) FA
      WRITE(6,*) FA
      END




      PROGRAM REEN
      REAL A,B,RA,RP,MU,VA,FPA,R,DV,V,G,M,CD,CL,K,Z1,Z2,
     +RO1,L,Y,RO2,DRO,BA,S,J,J2,RB,Z,LI,LF,C,D,HA,HP,
     +DV1,DV2,VAB,FPAD,VH,STOP,EP,CP,INV,NP,NM,FA,FV,
     +ZM,GO,TT,Q,PS,SI,SS,VE,RE,N,TS,DA,DA1,DA2
C
C
C     THE PURPOSE OF THIS PROGRAM IS TO GENERATE THE REE
C     NTRY PARAMETERS FROM A VEHICLE RETURNING FROM LOW
C     EARTH ORBIT.  THE INPUTS FOR THE PROGRAM ARE THE
C     ORBIT'S APOGEE AND PERIGEE, THE DESIERED REENTRY
C     FLIGHT PATH ANGLE (MEASURED POSITIVE BELOW THE HORI
```

```
C       ZON), THE DESIRED REENTRY VELOCITY, THE MASS OF THE
C       VEHICLE, THE REFERENCE AREA, THE ALTITUDE ABOVE THE
C       EARTH'S SURFACE TO START AND STOP THE CALCULATIONS,
C       AS WELL AS THE INTERVAL STEP SIZE.  THE OUTPUT IS THE
C       ALTITUDE, LOAD (IN G'S) VELOCITY,FLIGHT PATH ANGLE,
C       BALLISTIC COEFFICIENT, DENSITY, AND CONSERVATION PAR
C       AMETER.
C
C
C       THIS PROGRAM MUST BE USED IN CONJUNCTION WITH OTHER
C       PROGRAMS AND INPUT FILES.   THE PROGRAM INPUT.FOR
C       WILL CREATE THE INPUT FILES ORB.DAT AND LTD.DAT CON
C       TAINING ORBITAL DATA AND LIFT TO DRAG DATA, RESPEC
C       TIVELY.  THE PROGRAM OUTPUT IS PLACE INTO A FILE
C       CALLED LOAD.DAT.  THE FILE DEN.DAT MUST BE PRESENT TO
C       COMPUTE THE ATMOSPHERIC DENSITY.
C
C
C       SEVERAL SUBROUTINES ARE EMBEDDED IN THIS PROGRAM.
C       SUBROUTINE DEN CALCULATES THE DENSITY OF THE ATMO
C       SPHERE AT A GIVEN ALTITUDE. SUBROUTINE DELT THEN COM
C       PUTES THE DIFFERENCE BETWEEN TWO DENSITIES.  THE
C       INTEGRATIONS ARE CARRIED OUT WITH RESPECT TO DENSITY
C       AND THE DELTA IS REQUIRED FOR THE ALGORITHM.  SCAN IS
C       A SUBROUTINE WHICH SCANS THE LIFT AND DRAG TABLE TO
C       RETRIEVE THE APPROPRIATE COEFFICIENTS.  SUBROUTINES
C       LAM AND CGAM PERFORM THE ACTUAL INTEGRALS.
C
C       NOMENCLATURE:
C
C       A SCRATCH PAD
C       B SCRATCH PAD
C       BA BETA, THE BALLISTIC COEFFICIENT, LBS FORCE/FT
C          SQUARED
C       C SCRATCH PAD
C       CD DRAG COEFFICIENT
C       CL LIFT COEFFICIENT
C       D SCRATCH PAD
C       DRO DIFFERENCE IN DENSITY ACROSS THE INTEGRATION
C          INTERVAL
C       DV DELTA VELOCITY AT APOGEE TO BEGIN REENTRY ORBIT
C       FPA FLIGHT PATH ANGLE, RADIANS
C       FPAD FLIGHT PATH ANGLE, DEGREES
C       G ACCELERATION DUE TO GRAVITY FT/S SQUARED
C       GO ACCELERATION DUE TO GRAVITY AT SEA LEVEL
C       HA HEIGHT ABOVE THE EARTH'S SURFACE AT APOGEE, FT
C       HP HEIGHT AT PERIGEE, FT
C       INV  INTERVAL OVER WHICH INTEGRATION OCCURS, FT
C       J COUNTER
C       J2 COUNTER
C       K LIFT TO DRAG RATIO
```

```
C       L LAMDA, NON-DIMENSIONAL VELOCITY PARAMETER V
C          SQUARED/GO*RE
C       LF LAMDA VALUE AT THE END OF INTEGRATION INTERVAL
C       LI LAMDA VALUE AT START OF INTEGRATION INTERVAL
C       M MASS OF VEHICLE, SLUGS
C       MU GM, GRAVITATIONAL PARAMETER.  IN FT CUBED/S
C          SQUARED
C       N MAGNITUDE OF THE TOTAL VEHICULAR LOADING, G'S
C       NM MAXIMUM G'S COMPUTED
C       NP PREVIOUS VALUE OF N
C       PS PSI, THE ROLL ANGLE, DEGREES
C       Q FLAG TO INDICATE ASCENT OR DESCENT
C       R RADIUS OF VEHICAL AT ENTRY POINT, FT
C       RA RADIUS AT APOGEE FROM EARTH CENTER, IN FT
C       RE RADIUS OF THE SPHEREICAL EARTH, FT
C       RO1 DENSITY AT START OF NUMERICAL INTEGRATION SLUG/FT
C          CUBED
C       RO2  DENSITY AT END OF INTEGRATION INTERVAL
C       RP RADIUS AT PERIGEE
C       S REFERENCE AREA, FT SQUARED
C       SI   PSI, ROLL ANGLE, RADIANS
C       SS SINE OF PSI
C       STOP LOWEST HEIGHT TO INETGRATE, FT
C       V VELOCITY OF VEHICLE DURING DESCENT, FT/S
C       VA VELOCITY AT APOGEE FT/S
C       VAB VELOCITY AT APOGEE AFTER BURNOUT FT/S
C       VE VELOCITY AT ENTRY POINT, FT/S
C       VH SCRATH PAD VELOCITY
C       Y THE COSINE OF THE FLIGHT PATH ANGLE
C       ZM HEIGHT AT WHICH MAXIMUM G'S OCCUR, FT
C       Z1 HEIGHT AT START OF INTEGRATION INTERVAL, FT
C       Z2 HEIGHT AT END OF INTEGRATION INTERVAL, FT
C
C
C
C       OPEN(6,FILE='ORBT.DAT',STATUS='OLD')
        REWIND 6
        MU=1.407647E+16
        GO=32.14824
        Q=1.0
C
C
        READ (6,*) Z1
        READ (6,*) A,B
        READ (6,*) FPAD
        READ (6,*) FV,VE
        READ (6,*) M
        READ (6,*) S
        READ (6,*) INV
        READ (6,*) STOP
        READ (6,*) FA
```

```
      FPA=3.14159*FPAD/180
      IF (A.GT.B) THEN
         HA=A
         HP=B
      ELSE
         HA=B
         HP=A
      ENDIF
      RA=(3443.9+HA)*6076
      RP=(3443.9+HP)*6076
      A=1/RA
      B=1/(RA+RP)
      VA=SQRT(2*MU*(A-B))
      R=Z1+3443.9*6076
      A=2*MU*((1/R)-(1/RA))
      Y=COS(FPA) B=RA/(R*Y)
      C=B**2 D=C-1 B=(A/D)
      VAB=SQRT(B) DV1=VAB-VA
      V=(RA*VAB)/(R*Y)
      IF (FV.EQ.1) THEN
         V=VE
         DV2=V-VE
      ELSE
         DV2=0
      ENDIF
      DV=DV1+DV2
      WRITE(*,10) VA,VAB,DV,V
10    FORMAT(2X,'VA=',F8.0,2X,'VAB=',
     + F8.0,2X,'DV=',F8.0,2X,'V=',F8.0)
      OPEN (4,FILE='LOAD.DAT',STATUS='OLD')
      CALL DEN (Z1,RO1)
      RE=3443.9*6076
      G=MU/((Z1+RE)**2)
      LI=(V**2)/(RE*GO)
      Z2=Z1-INV 1000
      CALL SCAN(Z2,CL,CD,K,PS)
      G=MU/((Z2+RE)**2)
      BA=(M*G)/(CD*S) SI=PS*3.14159/180
      SS=SIN(SI)
      IF (FA.EQ.0) THEN
         A=G*RO1*K*SS/(2*BA)
         B=(1/(RE+Z1))+G*SIN(FPA)/(LI*GO*RE)
         ALF=ASIN(A/B)
      ELSE
         ALF=0.0
      ENDIF
      CALL DELT(Z2,RO1,RO2,DRO)
      CALL LAM (RO1,FPA,BA,LI,LF,DRO,G,ALF)
      L=(LI+LF)/2
      CALL CGAM(FPA,K,BA,L,DRO,RO1,
     +Y,G,Z1,Q,SI,ALF)
```

```
      VH=V
      V=(LF*RE*GO)**0.5
      A=(SIN(FPA)*COS(ALF)+K*SIN(SI)*SIN(FPA)*SIN(ALF)
     + +K*COS(SI)*COS(FPA))*RO2*V*V/BA
      B=(1+K*K)*RO2*RO2*(V**4)/(4*BA*BA)
      N=(1-A+B)**0.5
      IF (N.GT.NM) THEN
         NM=N ZM=Z2
      ELSE
      ENDIF
      FPAD=FPA*180/3.14159
      WRITE(4,30) Z2,N,V,FPAD,K,BA,RO2,K
30    FORMAT(2X,F9.0,2X,F7.2,2X,F7.0,2X,F7.2,
     +2X,F7.2,2X,F7.2,2X,E11.6,2X,F7.2)
      RO1=RO2
      LI=LF
      Z1=Z2
      Z2=Z1-INV*Q
      J=J+1 J2=40000/INV
      IF (J.GE.J2) THEN
         WRITE(*,45) Z1
45       FORMAT(5X,F9.0)
         J=0
      ELSE
      ENDIF
      IF (Z1.GT.STOP) GOTO 1000
      WRITE(*,*) 'N MAX=',NM,' Z MAX=',ZM
      CLOSE(6,STATUS='KEEP')
      CLOSE(4,STATUS='KEEP')
      END
C
C
C
C
      SUBROUTINE DELT (Z,RO1,RO2,DRO)
      REAL Z,RO1,RO2,DRO,H
C
      CALL DEN (Z,RO2)
      DRO=RO2-RO1
      END
C
C
C
C
      SUBROUTINE SCAN (Z1,CL,CD,K,PS)
      REAL Z1,CL,CD,K,TCL,TK,TCD,TZ,TP
C
      IF (Z1.NE.0) THEN
         OPEN (2,FILE='LTD.DAT',STATUS='OLD')
         REWIND 2
100      READ (2,*) TZ,TCL,TCD,TK,TP
```

```
            IF (Z1.LE.TZ) THEN
               CL=TCL
               CD=TCD
               K=TK
               PS=TP
            ELSE
               GOTO 200
            ENDIF
            GOTO 100
200         CLOSE(2,STATUS='KEEP')
         ELSE
         ENDIF
         END
C
C
C
C
         SUBROUTINE LAM (TRO,FPA,BA,LA,L,DRO,G,ALF)
         REAL TRO,FPA,BA,L,DRO,RE,G,
        +S,H,D,C,LA,GO,CA,ALF
         REAL*8 L1,L2,L3,L4,L5,L6,L7,R1,R2,R3,R4,
        +R5,R6,R7,TL,TL1,TL2,TL3,TL4,TL5,TL6,TL7,
        +RO,KRO
C
         GO=32.14824
         RO=TRO
         KRO=DRO
         RE=3443.9*6076
         CA=COS(ALF)
         S=SIN(FPA)
         H=21981.6
         D=(2*H*G)/(RE*GO)
         C=(G*H)/(BA*S*CA)
         R1=RO**(-1)
         R2=RO**(-2)
         R3=RO**(-3)
         R4=RO**(-4)
         R5=RO**(-5)
         R6=RO**(-6)
         R7=RO**(-7)
         L1=D*R1-C*LA
         L2=-1*D*R2-C*L1
         L3=2*D*R3-C*L2
         L4=-6*D*R4-C*L3
         L5=24*D*R5-C*L4
         L6=-120*D*R6-C*L5
         L7=720*D*R7-C*L6
         TL1=KRO*L1
         TL2=(KRO**2)*L2/2
         TL3=(KRO**3)*L3/6
         TL4=(KRO**4)*L4/24
```

```
      TL5=(KRO**5)*L5/120
      TL6=(KRO**6)*L6/720
      TL7=(KRO**7)*L7/5040
      TL=LA+TL1+TL2+TL3+TL4+TL5+TL6+TL7
      L=TL
      END
C
C
C
C
      SUBROUTINE CGAM(FPA,K,BA,L,DRO,TRO,
     +Y,G,Z1,Q,SI,ALF)
      REAL FPA,BA,L,DRO,TRO,Y,RE,H,K,
     +G,D,C,C1,C2,G0,Q,P,SI,CA,ALF
      REAL*8 RO,Y1,Y2,Y3,Y4,Y5,Y6,Y7,R1,R2,R3,R4,
     +R5,R6,R7,TY,TY1,TY2,TY3,TY4,TY5,
     +D2,D3,D4,D5,D6,D7,DD
C
      G0=32.14824
      P=COS(SI)
      RO=TRO
      DD=DRO
      RE=3443.9*6076
      Y=COS(FPA)
      CA=(COS(ALF))**2
      H=21981.6
      D=(K*G*H*P)/(2*BA*CA)
      R1=RO**(-1)
      R2=RO**(-2)
      R3=RO**(-3)
      R4=RO**(-4)
      R5=RO**(-5)
      R6=RO**(-6)
      R7=RO**(-7)
      D2=DD**2
      D3=DD**3
      D4=DD**4
      D5=DD**5
      D6=DD**6
      D7=DD**7
      C1=(RE+Z1)*L*CA
      C2=(RE/C1)-1
      C=(H*C2)/(RE+Z1)
      Y1=D/C-R1*Y
      Y2=R2*Y-R1*Y1
      Y3=-2*R3*Y+2*R2*Y1-R1*Y2
      Y4=6*R4*Y-6*R3*Y1+3*R2*Y2-R1*Y3
      Y5=-24*R5*Y+24*R4*Y1-12*R3*Y2+4*R2*Y3-R1*Y4
      Y6=120*R6*Y-120*R5*Y1+60*R4*Y2-20*R3*Y3
     ++5*R2*Y4-R1*Y5
      Y7=-720*R7*Y+720*R6*Y1-360*R5*Y2+120*R4*Y3
```

```
     +-30*R3*Y4+6*R2*Y5-R1*Y6
      TY1=(DRO)*Y1
      TY2=D2*Y2/2
      TY3=D3*Y3/6
      TY4=D4*Y4/24
      TY5=D5*Y5/120
      TY6=D6*Y6/720
      TY7=D7*Y7/5040
      TY=Y/C+TY1+TY2+TY3+TY4+TY5+TY6+TY7
      Y=TY*C
      IF (Y.GT.1) THEN
         E=2-Y FPA=-1*(ACOS(E))
         IF (F1.EQ.0) THEN
            WRITE(*,*) 'SKIP!'
            F1=1
         ELSE
         ENDIF
         Q=-1.0
      ELSE
         IF (FPA.EQ.1) FPA = .999999999999
         FPA=ACOS(Y)
         Q=1.0
      ENDIF
      END
C
C
C
      SUBROUTINE DEN(Z,RHO)
      REAL Z,RHO
      REAL*8 RE,K,A1,A2,A3,A4,A5,A6,
     +B1,B2,B3,B4,B5,B6,C1,C2,C3,C4,
     +RO,RI,Z1,Z2,P,Q,TZ1,TP,TQ,TRI,MW
C
C
      Z2=Z
      OPEN(3,FILE='DEN.DAT',STATUS='OLD')
      IF (Z2.GT.360000) THEN
         D1=Z2**(-2.7)
         D2=2.88E015*D1-13.289
         RO=5.11482*(10**(D2))
         GOTO 300
      ELSE
      ENDIF
      REWIND 3
100   READ (3,*) TZ1,TP,TQ,TRI,MW
      IF (TZ1.LE.Z2) THEN
         Z1=TZ1
         P=TP
         Q=TQ
         RI=TRI
      ELSE
```

```
      GOTO 100
   ENDIF
   RE=3443.9*6076
   K=32.14824/(49621.3*2/MW)
   A1=1+(Z1/RE)
   A2=1+(Z2/RE)
   A3=((Q**2)-(2*Q*P/RE)+((P/RE)**2))**(-1)
   A4=P+Q*Z1
   A5=P+Q*Z2
   A6=(Q-2*P/RE)
   B1=RE*A1*A2
   B2=(Z1-Z2)*A6
   B3=B2/B1
   B4=(A1/A2)**2
   B5=(A5/A4)**2
   B6=Q*DLOG(B4*B5)
   C1=B6+B3
   C2=-K*C1*A3
   C3=DEXP(C2)
   C4=A4*C3/A5
   RO=RI*C4
300 RHO=RO
   CLOSE(3,STATUS='KEEP')
   END
```

VITA

Steven W. Moss was born in San Rafael, California on April 12, 1957. He attended elementary schools in the Dixie (San Rafael) and Los Angeles City Unified School Districts, and graduated from Chatsworth High School in June, 1975. In 1979 he entered California State University, Northridge and in January 1983, received the degree of Bachelor of Science in Business Administration, Finance Option. In September 1983 he attended The Air Force Institute of Technology, Wright-Patterson Air Force Base, Ohio, graduating March 1985, receiving a Bachelor of Science in Aeronautical Engineering. From April 1985 to June 1987, he worked at The National Aeronautics and Space Administration, Langley Research Center, Hampton, Virginia, as a Wind Tunnel Test Project Engineer. In October of 1987 he entered The University of Tennessee, Knoxville and in May, 1991 received a Master of Science degree in Aerospace Engineering.

He is presently a Captain in The United States Air Force, stationed at The Arnold Engineering Development Center, Arnold Air Force Base, Tennessee, serving as an Aeronautical Systems Test Project Manager.